Journal of Medicinal Chemistry

Article

pubs.acs.org/jmc

(*Z*)-1-Aryl-3-arylamino-2-propen-1-ones, Highly Active Stimulators of Tubulin Polymerization: Synthesis, Structure–Activity Relationship (SAR), Tubulin Polymerization, and Cell Growth Inhibition Studies

M. V. Ramana Reddy,*[,†] Balaiah Akula,[‡,§] Stephen C. Cosenza,[†,§] Clement M. Lee,[†] Muralidhar R. Mallireddigari,[‡] Venkat R. Pallela,[‡] D. R. C. Venkata Subbaiah,[†] Andrew Udofa,[†] and E. Premkumar Reddy*[,†]

[†]Department of Oncological Sciences, Mount Sinai School of Medicine, Icahn Medical Institute, 1425 Madison Avenue, New York, New York 10029-6514, United States

[‡]Department of Medicinal Chemistry, Onconova Therapeutics Inc., 375 Pheasant Run, Newtown, Pennsylvania 18940, United States

ABSTRACT: Tubulin, the major structural component of microtubules, is a target for the development of anticancer agents. A series of (*Z*)-1-aryl-3-arylamino-2-propen-1-one (**10**) were synthesized and evaluated for antiproliferative activity in cell-based assay. The most active compound (*Z*)-1-(2-bromo-3,4,5-trimethoxyphenyl)-3-(3-hydroxy-4-methoxyphenylamino)prop-2-en-1-one (**10ae**) was tested in 20 tumor cell lines including multidrug resistant phenotype and was found to induce apoptosis in all these cell lines with similar GI_{50} values. Flow cytometry studies showed that **10ae** arrested the cells in G2/M phase of cell cycle. In addition to G2/M block, these compounds caused microtubule stabilization like paclitaxel and induced apoptosis via activation of the caspase family. The observations made in this investigation demonstrate that (*Z*)-1-Aryl-3-arylamino-2-propen-1-one (**10**) represents a new class of microtubule-stabilizing agents.

INTRODUCTION

Tubulin-containing structures, such as microtubules are important for the formation of the mitotic spindle during the process of mitosis. They play a critical role in cell growth, division, and cytoskeletal organization of normal and tumor cells as well as being implicated in motility, shape, and intracellular transport.[1] Microtubules are hollow tubes of α- and β-tubulin heterodimers that polymerize parallel to a cylindrical axis. Tubulin binding molecules interfere with the dynamic instability of microtubules and thereby disrupt microtubules, inducing cell cycle arrest in the M-phase, forming abnormal mitotic spindles resulting in the apoptotic cell death.[2] A number of natural compounds (see Chart 1), such as paclitaxel (**A**), epothilone (**B**), vinblastine (**C**), combretastatin A-4 (CA4) (**D**), dolastatin 10 (**G**), and colchicine (**H**), attack microtubules by interfering with the dynamics of tubulin polymerization and depolymerization, resulting in mitotic arrest.[3] However, many clinically useful chemotherapy drugs face substantial limitations such as drug resistance, high systemic toxicity, complex syntheses, and isolation procedures. This has encouraged scientists to develop new antimitotic agents. Recent studies have reported compounds targeting the colchicine-binding domain of β-tubulins that can act as vascular-disrupting agents, rapidly depolymerizing microtubules of newly formed vasculature to block the blood supply to tumors,[4] while leaving blood supply to healthy cells intact. These compounds include drug candidates combretastatin A-4P (CA4P) (**E**), Oxi4503, R, $R_1 = OPO_3Na_2$ (**F**), ZD6126 (**I**), which are shown in Chart 1.

The encouraging antivascular activity of compound **E** has stimulated significant interest in exploring new antitublin agents. A variety of synthetic small molecules have been reported as inhibitors of polymerization, which compete with the colchicine-binding site of tubulin.[5] Structurally, they involve various heteroaromatic cores, for instance including the benzothiophene,[6] benzofuran,[7] imidazole,[8] thiozole,[9] and oxadiazoline[10] moieties. A number of indole-based compounds, for example, 2-aroylindoles,[11] 3-aroylindoles,[12] 3-aroyl-2-phenylindoles,[7] 3-arylthioindoles-2-carboxylate,[13] and indolyl-3-glyoxamides,[14] have shown strong antiproliferative and tubulin depolymerizing activity.

Compounds like paclitaxel promote tubulin polymerization into microtubules and block microtubule dynamics, leading to abnormal mitosis and subsequent apoptosis.[15,16] Paclitaxel was the first microtubule-stabilizing agents (MSA) discovered.[17] It promotes the in vitro polymerization of tublin in the presence of guanosine triphosphate (GTP), which is normally required for microtubules assembly, and in cells, paclitaxel induces microtubule stabilization, leading to the formation of characteristic microtubule bundles.[18]

Three nontaxoid compounds have also been shown to stabilize microtubules. The macrolides epothilone A and epothilone B (**B**) from the bacterium *Sorangium cellulosum*,[19] and discodermolide (**J**) from the marine sponge *Discodermia dissolute*,[20] share with paclitaxel the ability to arrest cells in mitosis, cause formation of bundles of intracellular micro-

Received: February 8, 2012
Published: May 15, 2012

Chart 1. Examples of Tubulin Interacting Agents

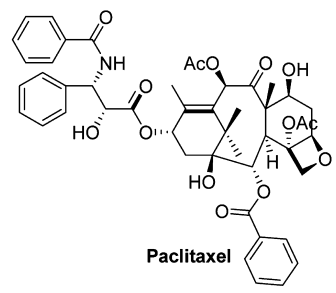

Paclitaxel

A

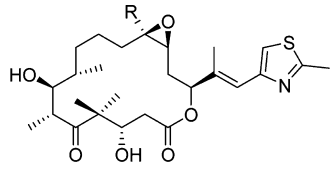

Epothilone A: R = H
Epothilone B; R = CH_3

B

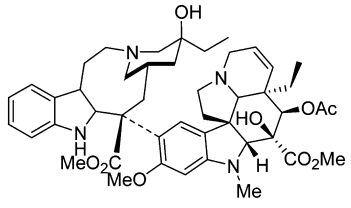

Vinblastine

C

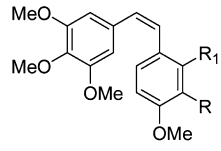

D: Combretastatin A-4 (CA4), R = OH; R_1 = H
E: Combretastatin A-4P (CA4P) R = OPO_3Na_2, R_1 = H
F: Oxi4503, R, R_1 = OPO_3Na_2

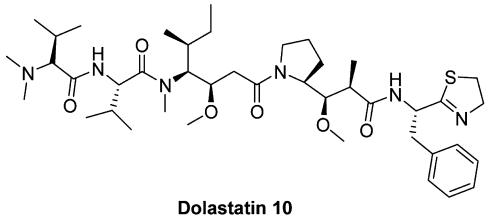

Dolastatin 10

G

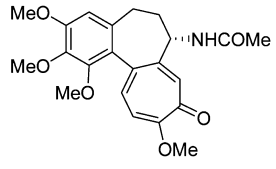

Colchicine

H

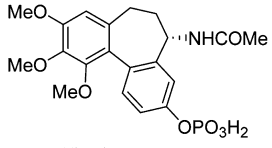

ZD6126

I

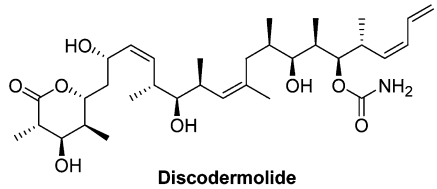

Discodermolide

J

tubules in nonmitotic cells, and induce the formation of hyperstable tubulin polymers.

A large number of small molecules have been described in the literature which inhibit tubulin polymerization in vitro and in vivo, resulting in the arrest of the cells in mitosis, ultimately leading to apoptosis. So far only two reports have described small synthetic molecules that stimulate tubulin polymerization and microtubule stabilization.[21,22] In this paper, we describe the synthesis, structure−activity relationship (SAR), and mode of action of a new series of (*Z*)-1-aryl-3-arylamino-2-propen-1-one (**10**) that stimulate tubulin polymerization and stabilizes microtubules.

Chemistry. The synthesis of target compounds (*Z*)-1-aryl-3-arylamino-2-propen-1-one (**10**) is illustrated in Scheme 1. Arylaldehydes **1**, **2**, **3**, and **6** were treated with ethynylmagnesium bromide in dry tetrahydrofuran (THF) at 0 °C to room temperature, producing 1-aryl-2-propyn-1-ol (**7**). Oxidation of **7** with 2-iodoxybenzoic acid (IBX) in the presence of dimethyl sulfoxide (DMSO) gave 1-aryl-2-propyn-1-one (**8**). Condensation of **8** with aryl amines (**9**) in ethanol at room temperature resulted in the formation of (*Z*)-1-aryl-3-arylamino-2-propen-1-one (**10**) in good yields.

Some of the substituted arylaldehydes (**2**, **3**, **6**), which are not commercially available, were synthesized as shown in the Schemes 2, 3, and 4. Chlorination of 3,4,5-trimethoxybenzaldehyde (**1c**) with sulfuryl chloride (SO_2Cl_2) in the presence of dichloromethane (CH_2Cl_2) afforded 2-chloro-3,4,5-trimethoxybenzaldehyde, **2** (Scheme 2). Similarly, the corresponding bromo compound **3** was obtained according to methods reported in literature.[23] Bromination of 3,4,5-trimethoxybenzaldehyde (**1c**), with *N*-bromosuccinimide (NBS) in chloroform at reflux temperature for 3 h, afforded 2-bromo-3,4,5-trimethoxybenzaldehyde, **3** (Scheme 3), whereas the 2-nitro-3,4,5-trimethoxybenzaldehyde, **6**, resulted by the oxidation of (3,4,5-trimethoxy-2-nitrophenyl)methanol (**5**) with manganese dioxide (MnO_2) in the presence of chloroform ($CHCl_3$) at room temperature for 48 h. **5**, in turn, was obtained by reduction of methyl 3,4,5-trimethoxy-2-nitrobenzoate (**4**) with

dx.doi.org/10.1021/jm300176j | *J. Med. Chem.* 2012, 55, 5174−5187

Scheme 1. Synthesis of (*Z*)-1-Aryl-3-arylamino-2-propen-1-one from 1-Aryl-2-propyn-1-one[a]

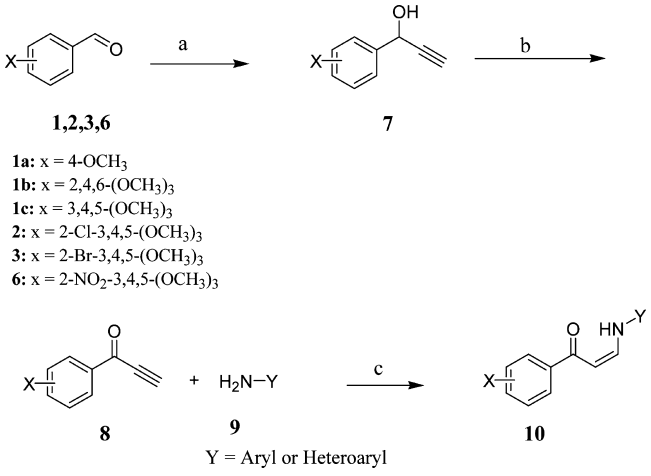

[a]Reagents and conditions: (a) ethynylmagnesium bromide, THF, 0 °C−rt, 8−9 h, 60−70%; (b) 2-iodoxybenzoic acid, DMSO, rt, 5 h, 70−72%; (c) ethanol, rt, 4 h, 60−82%.

Scheme 2. Synthesis of 2-Chloro-3,4,5-trimethoxybenzaldehyde[a]

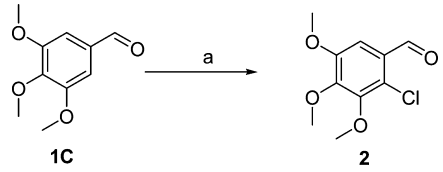

[a]Reagents and conditions: (a) sulfuryl chloride, dichloromethane, rt, 2 h, 60%.

Scheme 3. Synthesis of 2-Bromo-3,4,5-trimethoxybenzaldehyde[a]

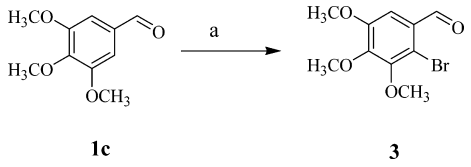

[a]Reagents and conditions: (a) NBS, chloroform, reflux, 3 h, 97%.

diisobutylaluminum hydride (DIBAH) in the presence of toluene at −50 °C (Scheme 4).

Structure−Activity Relationships (SAR). After the synthesis of these compounds, their in vitro cytotoxicity was assessed using two different human tumor cell lines derived from human prostate (DU145) and leukemic (K562) cancers. The results of the study are presented in Table 1. These studies reveal that the cytotoxicity of the 1-aryl-3-arylamino-2-propen-1-ones (**10**) is totally dependent on the nature and position of the substituents present on the two aromatic rings. For the purpose of structure−activity relationship, we have selected a few compounds from a library of enaminones synthesized in our laboratory. The cytotoxicity data (Table 1 and data not shown) clearly shows that the molecules are inactive when both aromatic rings are mono substituted (**10a**). A moderate cytoxicity was observed when benzoyl aromatic ring was tri substituted at third, fourth, and fifth positions with methoxy groups and anilino ring with a methoxy at second position (**10k**). A 5-fold increase in the activity was observed in **10k** when the 2-methoxy group on the anilino ring was relocated to fourth position (**10l**). When the pattern of substitution is

Scheme 4. Synthesis of 2-Nitro-3,4,5-trimethoxybenzaldehyde[a]

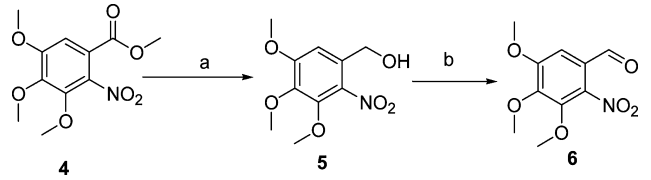

[a]Reagents and conditions: (a) anhydrous toluene, diisobutylaluminum hydride, −50 °C, 30 min, 55%; (b) chloroform, manganese dioxide, rt, 48 h, 63%.

Table 1. In Vitro Cytotoxicity of (*Z*)-1-Aryl-3-arylamino-2-propen-1-one 10[a]

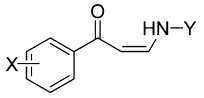

			IC_{50} (μM)	
compd	X	Y	DU145	K562
10a	4-OCH_3	4-OCH_3-C_6H_4	75	100
10b	4-OCH_3	3,4,5-$(OCH_3)_3$-C_6H_2	50	75
10c	2,4,6-$(OCH_3)_3$	4-OCH_3-C_6H_4	75	75
10d	2,4,6-$(OCH_3)_3$	2-OH-C_6H_4	25	75
10e	2,4,6-$(OCH_3)_3$	4−Cl-C_6H_4	25	25
10f	2,4,6-$(OCH_3)_3$	2,4-$(OCH_3)_2$-C_6H_3	75	75
10g	2,4,6-$(OCH_3)_3$	2,4,6-$(OCH_3)_3$-C_6H_2	75	50
10h	2,4,6-$(OCH_3)_3$	3,4,5-$(OCH_3)_3$-C_6H_2	35	75
10i	3,4,5-$(OCH_3)_3$	2-OH-C_6H_4	0.25	0.5
10j	3,4,5-$(OCH_3)_3$	3-OH-C_6H_4	0.75	0.5
10k	3,4,5-$(OCH_3)_3$	2-OCH_3-C_6H_4	2.5	2.5
10l	3,4,5-$(OCH_3)_3$	4-OCH_3-C_6H_4	0.5	0.5
10m	3,4,5-$(OCH_3)_3$	4-Cl-C_6H_4	0.5	0.25
10n	3,4,5-$(OCH_3)_3$	4-OCF_3-C_6H_4	3	20
10o	3,4,5-$(OCH_3)_3$	4-CF_3-C_6H_4	0.5	0.5
10p	3,4,5-$(OCH_3)_3$	3-OH,4-OCH_3-C_6H_3	0.1	0.1
10q	3,4,5-$(OCH_3)_3$	3-NH_2,4-OCH_3-C_6H_3	0.1	0.25
10r	3,4,5-$(OCH_3)_3$	3-F,4-OCH_3-C_6H_3	0.25	0.25
10s	3,4,5-$(OCH_3)_3$	3-Cl,4-OCH_3-C_6H_3	0.2	0.25
10t	3,4,5-$(OCH_3)_3$	2-Cl,5-OH-C_6H_3	0.75	2.5
10u	3,4,5-$(OCH_3)_3$	2,4,6-$(OCH_3)_3$-C_6H_2	75	50
10v	3,4,5-$(OCH_3)_3$	3,4,5-$(OCH_3)_3$-C_6H_2	40	25
10w	3,4,5-$(OCH_3)_3$	5-indolyl	0.2	0.5
10x	3,4,5-$(OCH_3)_3$	6-indolyl	0.1	0.2
10y	3,4,5-$(OCH_3)_3$	7-indolyl	2.5	2.5
10z	3,4,5-$(OCH_3)_3$	4-indazole	0.75	2.5
10aa	3,4,5-$(OCH_3)_3$	3-quinoline	0.5	0.75
10ab	3,4,5-$(OCH_3)_3$	2-CH_3,5-indolyl	0.6	0.75
10ac	2-Br,3,4,5-$(OCH_3)_3$	2-OH-C_6H_4	0.25	0.2
10ad	2-Br,3,4,5-$(OCH_3)_3$	4-OCH_3-C_6H_4	0.2	0.25
10ae	2-Br,3,4,5-$(OCH_3)_3$	3-OH,4-OCH_3-C_6H_3	0.06	0.1
10af	2-Br,3,4,5-$(OCH_3)_3$	5-indolyl	0.15	0.2
10ag	2-Cl,3,4,5-$(OCH_3)_3$	3-OH,4-OCH_3-C_6H_3	0.2	0.25
10ah	2-NO_2,3,4,5-$(OCH_3)_3$	4-OCH_3-C_6H_4	0.6	0.6

[a]Standard deviation for IC_{50} values were all within ±0.05 μM.

dx.doi.org/10.1021/jm300176j | J. Med. Chem. 2012, 55, 5174−5187

reversed by keeping 3,4,5-trimethoxy groups on the anilino ring and 4-methoxy group on the benzoyl ring (**10b**), the tumor cellular toxicity is reduced by more than 100-fold. These results show that the molecules with three methoxy groups on the benzoyl ring are more cytotoxic toward tumor cells than the compounds with three methoxy groups on the anilino ring. Once the benzoyl ring was identified as a correct moiety for tri substitution, we then looked at the position of the methoxy groups on the ring in modulating the cytotoxicity of the molecule. To analyze the role of the position of the methoxy groups, we have made a number of compounds with 2,4,6-trimethoxy substitutions on the benzoyl ring (**10c**, **10d**, **10e**, **10f**, **10g**, and **10h**). All the compounds with 2,4,6-trimethoxy benzoyl substituted lost the cytotoxicity effect on the tumor cells compared to the corresponding 3,4,5-trisubstituted benzoyl compounds. It clearly shows that **10l**, **10m**, and **10o**, which are 3,4,5 trimethoxy benzoyl, are 50-fold more active than **10c** and **10e**, which are 2,4,6-trimethoxy benzoyl enaminones. This confirms that the benzoyl ring of the enaminones presented in Table 1 require three methoxy groups at third, fourth, and fifth positions to attain maximum cytotoxicity toward cancer cells. To analyze the effect of additional substituents on the aniline aromatic ring, we have synthesized a number of analogues containing 3-hydroxy-4-methoxy (**10p**), 3-amino-4-methoxy (**10q**), 3-fluoro-4-methoxy (**10r**), 3-chloro-4-methoxy (**10s**), and 2-chloro-5-hydroxy (**10t**) groups; the cytotoxicity analyses of these analogues showed that the compounds with hydroxy and amino substituents at third position (**10p**, **10q**) exhibited the best activity in the series compared to the halo substituents (**10r**, **10s**, and **10t**). These compounds **10p** and **10q** are 5-fold more active than **10l**. In an attempt to further enhance the activity of the molecule, we have replaced aryl anilines with heteroaryl anilines. The replacement of heteroaryl anilines did not improve the cytotoxicity of the molecules (**10w**, **10x**, **10y**, **10z**, **10aa**, and **10ab**). After assigning third, fourth, and fifth positions to methoxy groups on benzoyl ring for optimum activity, we looked for the effect of a substituent at the ortho position of the benzoyl ring. It is clear from the cytotoxicity data of **10ac**, **10ad**, **10ae**, **10af**, **10ag**, and **10ah** that the inclusion of a halo or a nitro group at the ortho position moderately improved the activity of the molecules compared to the corresponding ortho-unsubstituted compounds. The SAR analysis of these compounds also shows that replacement of a methoxy (**10k** and **10l**), hydroxy (**10i** and **10j**) or chloro (**10m**) or trifluoro (**10o**) atoms or groups in these compounds with trimethoxy groups at 3,4,5 (**10v**) or 2,4,6 (**10u**) positions of anilino ring lead to the total loss of activity.

BIOLOGICAL RESULTS AND DISCUSSION

In Vitro Antitumor Effects of 10ae Compound. We next tested the activity of the most active compound (**10ae**) listed in Table 1 against different human tumor cell lines and, surprisingly, they were found to induce apoptosis of all of these cell lines with similar GI_{50} values (*selected* data shown in Table 2). The wide range of cell killing across multiple tumor types suggests that this compound is inducing tumor cell killing by inhibiting an intrinsically important process of tumor cell division.

10ae Compound Is Also Active against Drug Resistant Tumor Cell Line. Development of resistance to classical chemotherapeutic agents is widely observed in patients who have not responded or have relapsed after a first round of therapy and is the primary cause of treatment failure. Many microtubulin poisons such as paclitaxel, vincristine, and vinblastine are substrates for the multidrug resistant family members. To further investigate the activity of these compounds against MDR positive tumor types, we determined the IC_{50} value of **10ae** using a classical MDR-positive cell line. The results shown in Table 2 show a 96 h dose response of the uterine sarcoma cell line MES-SA and the multidrug resistant subline MES-SA/DX5[24] treated with **10ae**. This cell line has been shown to express high levels of P-glycoprotein and is resistant to a number of drugs including doxorubicin, paclitaxel, vincristine, vinblastine, etoposide, mitoxantrone, dactinomycin, and daunorubucin. The activity of our compound was then compared to the activity of paclitaxel (MDR sensitive drug). Our results show that the parental cell line was very sensitive to paclitaxel (IC_{50} 4 nM), but the MDR positive subline was greater than 100-fold resistant (IC_{50} 750 nM). When the two cell lines were treated with **10ae**, both the parental and the MDR positive cell lines were almost equally sensitive to the cell killing activity of the compound.

Table 2. Evaluation of 10ae against a Panel of Human Tumor Cell Lines[a]

cell line	tumor type	**10ae** (μM)
BT20	breast (ER−)	0.75
MCF-7	breast (ER+)	0.4
SK-BR-3	breast (ER−)	0.3
BT474	Breast (ER+)	0.1
DU145	prostate (AR−)	0.06
MIA-Paca2	pancreatic	0.8
A549	NSCLC	0.9
HeLa	cervical	0.2
COLO-320	colorectal	0.15
Panc-1	pancreatic	0.2
K562	CML	0.1
SK-MEL-28	melanoma	0.2
HTB-126	breast carcinoma	0.1
Caco-2	colorectal	0.25
Raji	Burkitt's lymphoma (B-cell)	0.2
SNU-5	gastric carcinoma	0.25
N87	gastric carcinoma	0.3
HCT-15	colorectal	0.04
MES-SA	sarcoma	0.25
MES-SA/DX5	resistant sarcoma	0.50

[a]Standard deviation for IC_{50} values were all within $\pm$0.025 μM.

Effects of 10ae on Cell Cycle Progression of Tumor Cells. Treatment of cancer cells with **10ae** results in a time-dependent rounding of the cells indicative of mitotic arrest.[25] To study the cell cycle effects of **10ae** treatment, we ran a series of experiments by fluorescence-activated cell sorting (FACS) and signal transduction studies using human prostate cancer cells. DU145 cells, which are androgen-negative prostate cancer cells, were treated with increasing concentrations of **10ae** for 24 h. Because these cells were one of the more sensitive cell lines tested, and because DU145 cells have a very predictable cell cycle time making them suitable for cell cycle analysis, these cells were used for the following experiment.[26−28] Cell cycle analysis performed by FACS analysis revealed that the cells accumulated in G2/M phase of the cell cycle in a concentration-dependent manner. Results presented in Figure 1 show that treatment with 0.25 μM of **10ae** resulted in the accumulation of tumor cells in the G2/M phase of the cell cycle

dx.doi.org/10.1021/jm300176j | J. Med. Chem. 2012, 55, 5174−5187

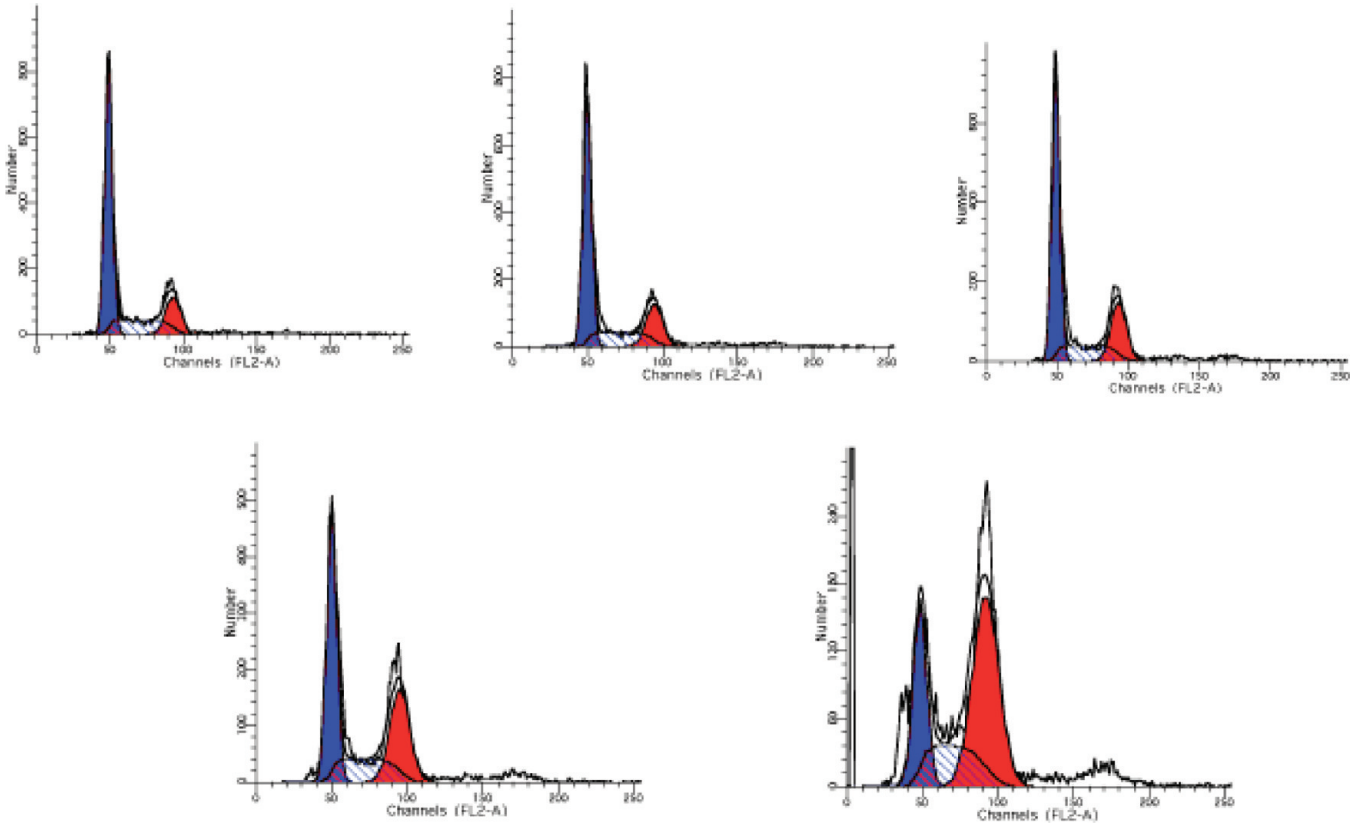

Figure 1. 10ae treatment of cancer cells results in G2/M arrest. DU145, human prostate cancer cells, were treated for 24 h with increasing concentrations of **10ae**, fixed, and stained with propidium iodide and analyzed for their DNA content by flow cytometry. G1 (2N), S-Phase (>2N < 4N), and G2/M (4N) cells are indicated solid blue, striped, and solid red, respectively. **10ae** treated cells become arrested in G2/M in a dose-responsive manner. DU145 cells were plated at a cell density of 1.0×10^6 cells per 100 mm dish. $N = 3$.

with a majority of cells showing G2/M arrest when treated with 0.5 μM concentration of the compound. The FACS analysis determined that the treated cells had greater than 2N amount of DNA but did not differentiate between G_2 and mitotic phases of the cell cycle. On the basis of these results, we next studied the effects of **10ae** on the phosphorylation status of proteins known to be important markers of mitotic arrest and spindle checkpoint activation. HeLa cells derived from a human cervical tumor which have been extensively studied as a model cell line for mitotic inhibitors[29] were treated with 1 μM concentration of **10ae** for various time points and the pattern of expression of histone H3 and its phosphorylated mitotic (ser10) form were analyzed. Phosphorylation of histone H3 (ser10) is a widely accepted indicator of mitotic arrest as well as a diagnostic tool for the mitotic index of tumors.[30−33] As shown in Figure 2, increased levels of phospho-histone H3 were observed within 6 h after treatment with maximal accumulation at 24 h (121-maximum-fold increase). Phosphorylation of BCL-2 has also been known to be a marker for mitosis,[34] and this protein became phosphorylated at the same time as histone H3 (88 fold). Concurrently to the accumulation of phospho-histone H3, the protein levels of both cyclin B1 (2.5 fold) and PLK-1(2.5 fold) increased after 6 h of treatment. The expression of these proteins is known to be closely linked to progression through mitosis.[35−37] Phosphorylation of BubR1 is a useful marker of mitotic arrest due to the activation of the spindle checkpoint,[38,39] so we next analyzed the phosphorylation status of this protein. Similar to histone H3 and Bcl-2, BubR1 (2.95-fold) became phosphorylated at 6 h following treatment of cancer cells with **10ae**. Taken together, these data strongly suggest that **10ae** treatment induces a mitotic arrest, with the activation of spindle checkpoint within 6 h of treatment.

Compound 10ae Induces Apoptosis in Tumor Cells. Tumor cells treated with **10ae** accumulated in the G2/M phase of the cell cycle in a dose-dependent manner and appeared to be unable to exit from this phase, leading to the activation of apoptotic pathways as judged by poly(ADP-ribose) polymerase-1 (PARP) cleavage,[40] which is a marker for caspase activation (Figure 3).

Compound 10ae Kills Tumor Cells by Stabilizing Microtubules. The polymerization of microtubules from purified tubulin can be monitored in vitro by measuring an increase in light scattering. This in vitro experiment removes complicating factors, such as microtubule-associated proteins (MAPs), which might be part of a putative target that leads to disruption of microtubules as observed with microscopy. To test our hypothesis that the target of (*Z*)-1-aryl-3-arylamino-2-propen-1-one (**10**) is tubulin, and not a MAP, we monitored the polymerization of tubulin after treatment with **10ag**, **10ah**, and **10ae** (Figure 4). In this experiment, paclitaxel, a microtubule stabilizer, enhanced the rate of tubulin polymerization, while vincristine, a microtubule destabilizer, prevented the polymerization of tubulin. Similar to paclitaxel, **10ag**, **10ah**, and **10ae** stabilized tubulin polymerization at 1 μM. Compound **10ae** was most potent in cytotoxicity assay compared to the other analogues, and also from Figure 4, **10ae** is superior to paclitaxel in that it causes more microtubule assembly at the

dx.doi.org/10.1021/jm300176j | *J. Med. Chem.* 2012, 55, 5174−5187

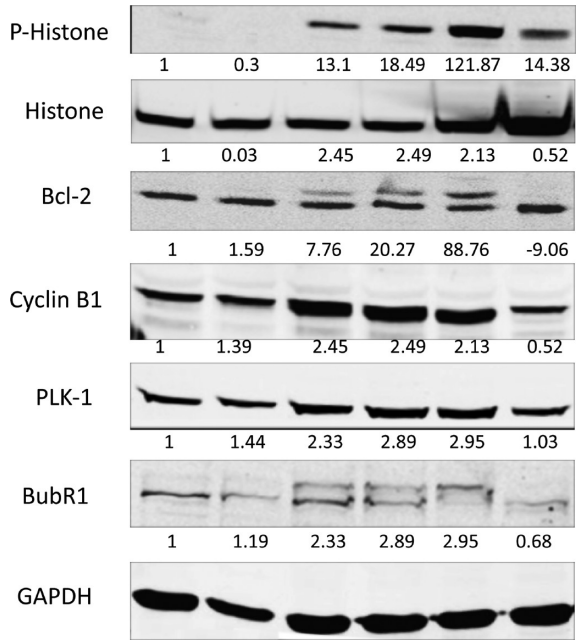

Figure 2. 10ae treatment induces mitotic arrest. HeLa cells were treated with 1 μM **10ae**, and cells were harvested for Western blotting at the indicted times. The blot was sequentially hybridized with antibodies specific for phospho-histone H3, histone H3, cyclin B1, PLK-1, Bub-R1, and GAPDH was used as a loading control. Phosphorylation of histone H3, BubR1, and Bcl-2 and the accumulation of mitotic specific proteins (cyclin B1 and PLK-1) indicates that **10ae** treatment induces a mitotic arrest, with cells starting to accumulate in mitosis by 6 h following treatment. Primary antibody dilutions were 1:1000 for all westerns, and 1:10000 for secondary antibodies. $N = 3$. The numbers below the panel represents the fold increase, calculated as described in the Experimental Section, of the respective protein or phosphoprotein.

Figure 3. 10ae treatment activates caspase-3 and induces apoptosis. HeLa cells were treated with 1.0 μM **10ae** for the indicated times, and protein lysates were resolved by SDS-PAGE and analyzed for caspase-3 activation by Western blotting using anti-PARP specific antibodies. PARP cleavage was observed starting at 24 h. This data indicates that the apoptosis pathway has been activated. Primary antibody dilutions were 1:1000 for all westerns and 1:10000 for secondary antibodies. $N = 3$.

same concentration (1 μM). Thus, the enaminone-based compounds stabilize the formation of microtubules in vitro.

Compound 10ae Treatment Induces Abnormal Mitotic Spindle Development. Because **10ae** was found to alter tubulin in vitro polymerization kinetics, we next examined the mitotic spindle apparatus in cancer cells treated with **10ae**. HeLa cells were treated with **10ae** for 18 h and fixed and stained for α-tubulin. Figure 5 shows that HeLa cells became arrested in mitosis and the mitotic cells had abnormal mitotic spindles. When cells were treated with the 0.25 μM of **10ae**, near the GI_{50} value, the mitotic cells displayed an atypical bipolar metaphase plate in which the tubulin appeared bundled at the poles and some chromosomes that were not attached aligned at the metaphase plate (see arrows). When the cells were treated with higher concentrations of **10ae**, the mitotic cells acquired multiple tubulin bundles (multipolar) without chromosomes aligned at the metaphase plate with more dispersion of the chromosomes. We compared the mitotic spindle phenotype to cells treated with paclitaxel, a tubulin stabilizer, and to cells treated with vincristine, a tubulin depolymerizer. As shown in Figure 5, **10ae** treatment is unique in its effect on mitotic spindle formation, in that although the mitotic cells are multipolar which is similar to paclitaxel, the intensity of the tubulin staining is lower and the chromosome spreads are different. At lower concentrations, **10ae** was similar to paclitaxel in that unbound chromosomes were observed outside the metaphase plate while higher concentrations resulted in a more dispersed chromosome spread with three or more tubulin bundles. When one compares **10ae** to vincristine treated cells, it is clear that **10ae** is not destabilizing tubulin because we do not observe complete loss of tubulin staining.

The effects of **10ae** treatment on tubulin stability can also be examined by analysis of the tubulin organization of nonmitotic interphase cells. Figure 6 shows that treatment with high concentrations of **10ae** did not result in an overall disruption of cytoplasmic microtubule organization as evident in cells treated with vincristine. The microtubule organization appeared to be somewhat shortened throughout the cytoplasm, but the overall protofilament structure was still intact. Paclitaxel treatment resulted in bundling of the microtubule fibers near the nucleus; this was not observed with **10ae** treatment. This data suggests that **10ae** treatment does not depolymerize tubulin but interferes with microtubule spindle development during mitosis without altering cytoplasmic microtubules, resulting in a mitotic block and cell death.

CONCLUSION

In this communication, we describe the synthesis of a series of (*Z*)-1-aryl-3-arylamino-2-propen-1-ones (**10**) molecules, which induce apoptotic death of a wide variety of human tumor cell lines at nanomolar concentrations by promoting tubulin polymerization and stabilizing microtubules. This is a first report that shows a group of small synthetic molecules (**10**) behave like paclitaxel and epothilones in tumor cell killing in the nanomolar range by promoting tubulin polymerization and microtubule stabilization in in vitro. Our studies show that the cytotoxic activity of the (*Z*)-1-aryl-3-arylamino-2-propen-1-ones (**10**) is completely dependent on the nature and position of the substituents on the two aromatic rings. These structure function studies show that a molecule with an aniline ring having 3-hydroxy, 4-methoxy groups and a benzoyl ring with a bromine atom at ortho and methoxy groups at 3-, 4-, and 5-positions (**10ae**) showed optimum biological activity. Biological evaluation of the activity of **10ae** shows that this compound is highly active against a wide variety of human tumor cell lines including those that are resistant to the activity of many of the currently used chemotherapeutic agents.

EXPERIMENTAL SECTION

Chemistry. *General Methods.* All reagents and solvents were obtained from commercial suppliers and used without further purification unless otherwise stated. Solvents were dried using standard procedures, and reactions requiring anhydrous conditions were performed under N2 atm. Reactions were monitored by thin layer chromatography (TLC) on preloaded silica gel F254 plates (Sigma-Aldrich) with a UV indicator. Column chromatography was performed with Merck 70-230 mesh silica gel 60 Å. Yields were of

dx.doi.org/10.1021/jm300176j | J. Med. Chem. 2012, 55, 5174−5187

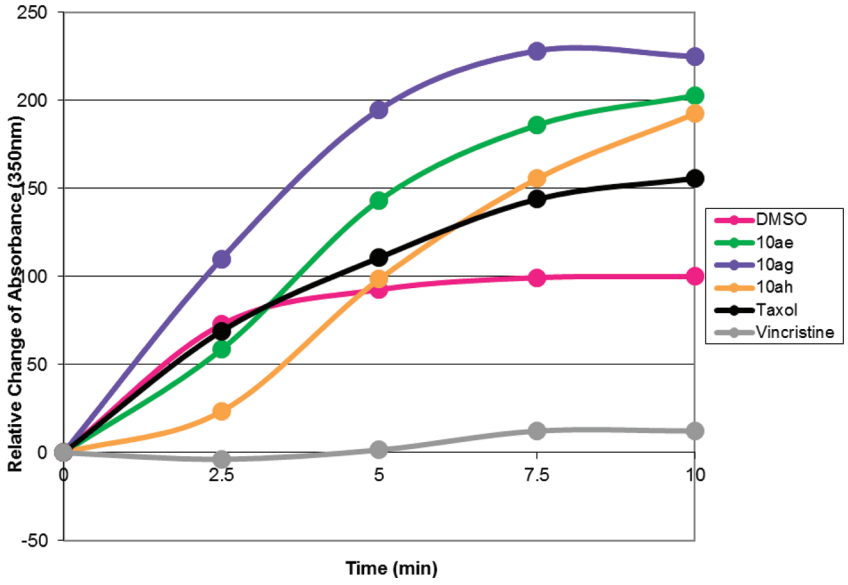

Figure 4. MAP-rich tubulin from bovine brain had been preincubated with various drugs (1 μM final) or vehicle dimethyl sulfoxide at room temperature for 5 min before guanosine triphosphate (GTP) was added to start the tubulin polymerization reactions. The reaction was monitored at various time points at OD350 nm at 37 °C. Tubulin polymerization enhancer (taxol) and inhibitor (vincristine) were included as controls.

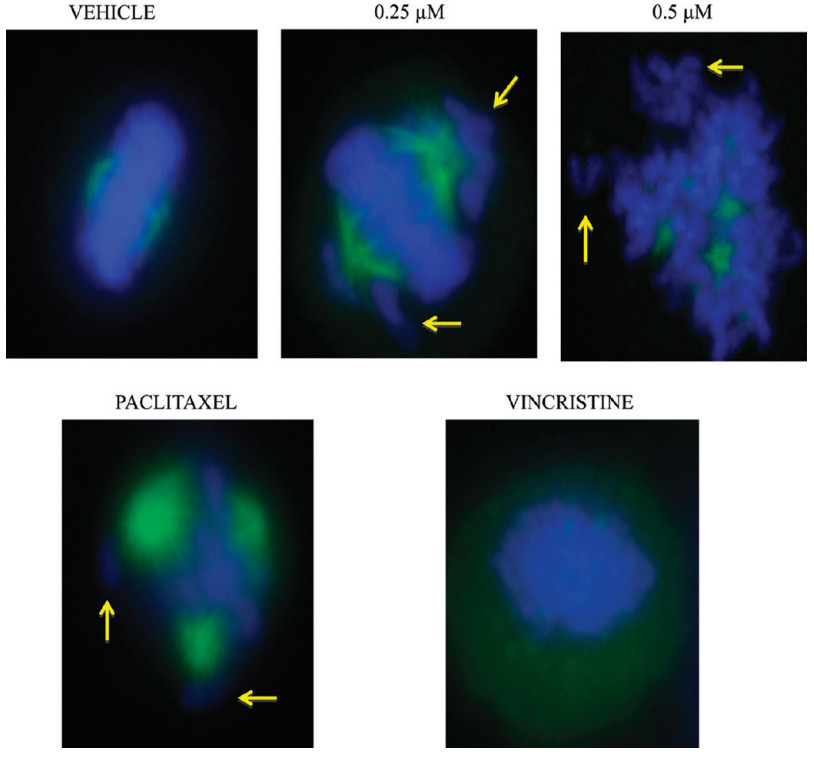

Figure 5. 10ae treatment results in abnormal microtubule spindle development. HeLa cells were treated with 0.25 or 0.5 μM of **10ae**, 0.005 μM paclitaxel, 0.005 μM vincristine, or DMSO for 18 h and fixed and stained with anti-α-tubulin-FITC specific antibodies (green) followed by DAPI to visualize chromosomes (blue). **10ae** and paclitaxel treatment resulted in abnormal mitotic cells with chromosomes not aligned at the metaphase plate (see arrows) without complete loss of tubulin polymers as observed in cells treated with vincristine. Cell density was 1.0×10^6 cells per 100 mm dish containing eight coverslips each.

purified product and were not optimized. Melting points were determined using an Electro Thermal Mel-Temp 3.0 micromelting point apparatus and are uncorrected. ^{1}H NMR spectra were obtained with a Bruker AM 300 and 400 MHz spectrometer. The chemical shifts are reported in parts per million (δ) downfield using tetramethylsilane ($SiMe_4$) as internal standard. Spin multiplicities are given as s (singlet), d (doublet), dd (double doublet), brs (broad singlet), m (multiplet), and q (quartet). Coupling constants (J values) were measured in hertz (Hz). All LC/MS data were gathered on an Agilent 1200 LC with Agilent 6410 triple quadrupole mass spectrometer detectors. The compound solution was infused into the electrospray ionization source operating positive and negative modes in methanol/water/TFA (50:50:0.1% v/v) at 0.4 mL/min. The sample cone (declustering) voltage was set at 100 V. The instrument was externally calibrated for the mass range m/z 100 to m/z 1000. The

dx.doi.org/10.1021/jm300176j | J. Med. Chem. 2012, 55, 5174−5187

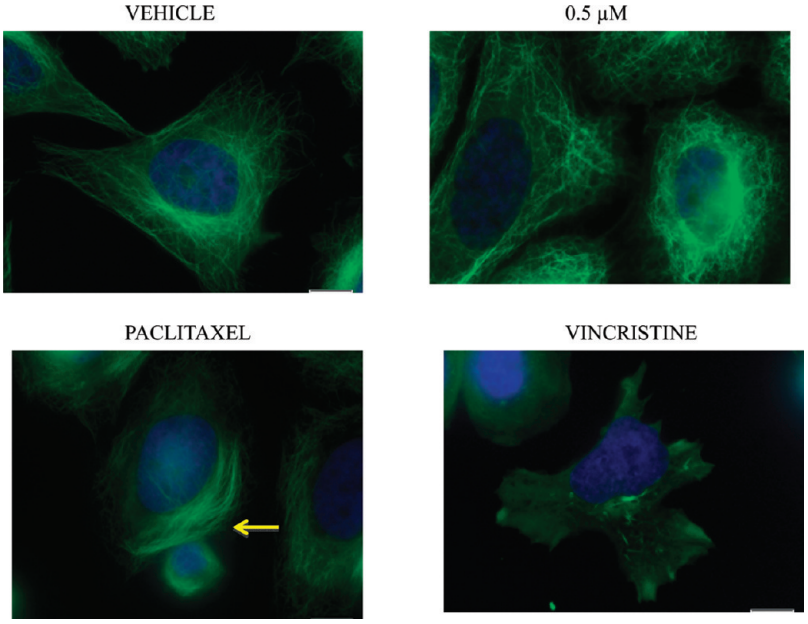

Figure 6. 10ae treatment does not alter cytoplasmic microtubules. High concentrations of **10ae** (0.5 μM) did not result in bundling of the cytoplasmic microtubules as seen with paclitaxel (0.005 μM) treatment (arrow) nor did **10ae** treatment depolymerize cytoplasmic microtubules as observed in cells treated with vincristine (0.005 μM). Cell density was 1.0×10^6 cells per 100 mm dish containing eight coverslips each.

purity of the final compounds was determined by HPLC and is 95% or higher unless specified otherwise.

*Synthesis of 2-Chloro-3,4,5-trimethoxybenzaldehyde (**2**).* 3,4,5-Trimethoxybenzaldehyde **1c** (1.0 g, 5 mmol) was dissolved in 25 mL of dichloromethane, and sulfuryl chloride (0.49 mL, 6.1 mmol) was added and stirred at 10 °C for 2 h. After reaction was completed (checked by TLC), the solvent was concentrated under vacuum and washed with hexane to get pure 2-chloro-3,4,5-trimethoxybenzaldehyde **2** with 60% yield; semi solid. ^{1}H NMR ($CDCl_3$, 300 MHz): δ 3.91 (s, 3H, OCH_3), 3.93 (s, 3H, OCH_3), 3.99 (s, 3H, OCH_3), 7.27 (s, 1H, Ar−H), 10.39 (s, 1H, H−C═O). MS found $(M + H)^+$ (m/z): 231.20. Calcd for $C_{10}H_{11}ClO_4$ m/z: 230.03.

*Synthesis of 2-Bromo-3,4,5-trimethoxybenzaldehyde (**3**).* To a solution of 3,4,5-trimethoxy benzaldehyde **1c** (5.0 g, 25.4 mmol) in 50 mL chloroform ($CHCl_3$) was added *N*-bromosuccinimide (5.44 g, 30.5 mmol). The solution was heated at reflux temperature for 3 h. After the reaction was completed by TLC, the reaction mixture was brought to room temperature, and the solution was washed with water and extracted with diethyl ether (Et_2O). The combined extracts were dried with anhydrous Na_2SO_4 and concentrated. The crude bromobenzaldehyde was recrystallized from hexanes and Et_2O to get pure white solid with 97% yield; mp 69−70 °C. ^{1}H NMR ($CDCl_3$, 300 MHz): δ 3.90 (s, 3H, OCH_3), 3.92 (s, 6H, OCH_3), 7.30 (s, 1H, Ar−H), 10.15 (s, 1H, H−C═O). MS found $(M + H)^+$ (m/z): 275.10. Calcd for $C_{10}H_{11}BrO_4$ m/z: 273.98.

*Synthesis of 3,4,5-Trimethoxy-2-nitrobenzaldehyde (**6**). . Step 1: Synthesis of (3,4,5-Trimethoxy-2-nitrophenyl)methanol (**5**).* Methyl 3,4,5-trimethoxy-2-nitrobenzoate **4** (1.5 g, 3.69 mmol) was dissolved in 20 mL of anhydrous toluene, cooled to −50 °C, and treated with a solution of diisobutylaluminum hydride (1.0 M solution in hexane, 4.6 mL, 4.6 mmol) over a period of 10 min. After 30 min, the reaction was quenched with 10 mL of methanol and brought to room temperature. The resulting reaction mixture was diluted with water and extracted with ethyl acetate. The extract was dried over anhydrous Na_2SO_4 and concentrated under vacuum to give (3,4,5-trimethoxy-2-nitrophenyl)-methanol **5**, which was purified by column chromatography (silica gel, 30% ethyl acetate in hexane, R_f = 0.33) as brown solid with 55% yield; mp 59−60 °C. ^{1}H NMR ($CDCl_3$, 300 MHz): δ 2.34 (brs, 1H, OH), 3.90 (s, 3H, OCH_3), 3.95 (s, 3H, OCH_3), 4.00 (s, 3H, OCH_3), 6.85 (s, 1H, Ar−H). MS found $(M + H)^+$ (m/z): 244.10. Calcd for $C_{10}H_{13}NO_6$ m/z: 243.07.

*Step 2: Synthesis of 3,4,5-Trimethoxy-2-nitrobenzaldehyde (**6**).* The compound **5** (1.0 g, 4.1 mmol) was dissolved in 50 mL of chloroform to which MnO_2 (2.14 g, 24.6 mmol) was added and stirred for overnight, and an additional portion of MnO_2 (0.53 g, 6.15 mmol) was added and stirred for 12 h. The solids were removed by filtration through a Celite pad and washed with chloroform. The chloroform was evaporated in vacuo to get pure compound **6** as brown solid with 63% yield; mp 64−65 °C. ^{1}H NMR ($CDCl_3$, 300 MHz): δ 3.91 (s, 3H, OCH_3), 3.93 (s, 6H, OCH_3), 7.15 (s, 1H, Ar−H), 9.80 (s, 1H, H−C═O). MS found $(M + H)^+$ (m/z): 242.20. Calcd for $C_{10}H_{11}NO_6$ m/z: 241.06.

*General Procedure for the Synthesis of 1-Aryl-2-propyn-1-ol (**7**).* A solution of aldehyde **1**−**6** (5 mmol) in dry tetrahydrofuran (THF) was added to a stirred solution of ethynylmagnesium bromide in THF (0.5 M solution, 7.5 mmol) at 0 °C. The solution was stirred at 0 °C for 2 h and then warmed to room temperature and stirred for another 6−7 h. Saturated aqueous ammonium chloride solution 5 mL was added, and the mixture was evaporated in vacuo and partitioned between ethyl acetate and saturated ammonium chloride solution. The organic layer was washed with brine, dried over anhydrous Na_2SO_4, and evaporated in vacuo to get pure compounds and were used for next step without further purification.

*1-(4-Methoxyphenyl)prop-2-yn-1-ol (**7a**).* Starting from 4-methoxybenzaldehyde **1a**, 70% of **7a** was obtained according to the method described in general procedure **7**; liquid. ^{1}H NMR ($CDCl_3$, 400 MHz): δ 2.65 (d, 1H, J = 2.2 Hz, ≡H), 3.79 (s, 3H, OCH_3), 5.37−5.40 (m, 1H, H-C-OH), 6.87−6.90 (m, 2H, Ar−H), 7.43−7.47 (m, 2H, Ar−H). MS found $(M - H_2O + H)^+$ (m/z): 145.20. Calcd for $C_{10}H_{10}O_2$ m/z: 162.07.

*1-(2,4,6-Trimethoxyphenyl)prop-2-yn-1-ol (**7b**).* Starting from 2,4,6-trimethoxybenzaldehyde **1b**, 65% of **7b** was obtained as brown solid according to the method described in general procedure **7**; mp 119−120 °C. ^{1}H NMR ($CDCl_3$, 400 MHz): δ 2.42 (d, 1H, J = 2.3 Hz, ≡H), 3.80 (s, 3H, OCH_3), 3.86 (s, 6H, OCH_3), 5.80−5.84 (m, 1H, H-C-OH), 6.14 (s, 2H, Ar−H). MS found $(M - H_2O + H)^+$ (m/z): 205.30. Calcd for $C_{12}H_{14}O_4$ m/z: 222.09.

*1-(3,4,5-Trimethoxyphenyl)prop-2-yn-1-ol (**7c**).* Starting from 3,4,5-trimethoxybenzaldehyde **1c**, 65% of **7c** was obtained as brown solid according to the method described in general procedure **7**; mp 51−52 °C. ^{1}H NMR ($CDCl_3$, 400 MHz): δ 2.62 (d, 1H, J = 2.1 Hz, ≡H), 3.83 (s, 3H, OCH_3), 3.86 (s, 6H, OCH_3), 5.39−5.54 (m, 1H, H-

dx.doi.org/10.1021/jm300176j | J. Med. Chem. 2012, 55, 5174−5187

C-OH), 6.77 (s, 2H, Ar−H). MS found $(M - H_2O + H)^+$ (m/z): 205.20. Calcd for $C_{12}H_{14}O_4$ m/z: 222.09.

*1-(2-Chloro-3,4,5-trimethoxyphenyl)prop-2-yn-1-ol (**7d**).* Starting from 2-chloro-3,4,5-trimethoxybenzaldehyde **1d**, 70% of **7d** was obtained as brown solid according to the method described in general procedure **7**; mp 65−66 °C. ^{1}H NMR ($CDCl_3$, 400 MHz): δ 2.66 (d, 1H, J = 2.4 Hz, ≡H), 3.89 (s, 3H, OCH_3), 3.90 (s, 6H, OCH_3), 5.79−5.80 (m, 1H, H-C-OH), 7.14 (s, 1H, Ar−H). MS found $(M - H_2O + H)^+$ (m/z): 239.10. Calcd for $C_{12}H_{13}ClO_4$ m/z: 256.05.

*1-(2-Bromo-3,4,5-trimethoxyphenyl)prop-2-yn-1-ol (**7e**).* Starting from 2-bromo-3,4,5-trimethoxybenzaldehyde **1e**, 70% of **7e** was obtained as brown solid according to the method described in general procedure **7**; mp 59−60 °C. ^{1}H NMR ($CDCl_3$, 400 MHz): δ 2.66 (d, 1H, J = 2.1 Hz, ≡H), 3.88 (s, 3H, OCH_3), 3.89 (s, 6H, OCH_3), 5.79−5.80 (m, 1H, H-C-OH), 7.18 (s, 1H, Ar−H). MS found $(M - H_2O + H)^+$ (m/z): 283.20. Calcd for $C_{12}H_{13}BrO_4$ m/z: 300.00.

*1-(3,4,5-Trimethoxy-2-nitrophenyl)prop-2-yn-1-ol (**7f**).* Starting from 2-nitro-3,4,5-trimethoxybenzaldehyde **1f**, 60% of **7f** was obtained as brown solid according to the method described in general procedure **7**; mp 75−76 °C. ^{1}H NMR ($CDCl_3$, 400 MHz): δ 2.50 (d, 1H, J = 2.2 Hz, ≡H), 3.72 (s, 3H, OCH_3), 3.77 (s, 3H, OCH_3), 3.80 (s, 3H, OCH_3), 5.42−5.52 (m, 1H, H-C-OH), 6.91 (s, 1H, Ar−H). MS found $(M - H_2O + H)^+$ (m/z): 250.20. Calcd for $C_{12}H_{13}NO_6$ m/z: 267.07.

*General Procedure for the Synthesis of 1-Aryl-2-propyn-1-one (**8**).* A solution of 2-iodoxy-benzoic acid (IBX) (12.5 mmol) in dimethyl sulfoxide (DMSO) (90 mL) was stirred for 5 min at room temperature until homogeneous. A solution of secondary alcohol **7** (5 mmol) in DMSO (5 mL) was added, and the mixture was stirred for 5 h. Water (10 mL) was added, and the mixture was stirred at room temperature for 10 min, cooled in ice, and partitioned between water and ethyl acetate. The mixture was filtered through Celite, and the aqueous layer was further extracted with ethyl acetate. The organic extracts were combined, washed with water followed by saturated sodium bicarbonate solutions and brine, dried over sodium sulfate, and evaporated in vacuo to get the pure product and was used for next step without further purification.

*1-(4-Methoxyphenyl)prop-2-yn-1-one (**8a**).* Starting from 1-(4-methoxyphenyl)prop-2-yn-1-ol **7a**, 72% of **8a** was obtained as pale-yellow solid according to the method described in above-mentioned general procedure **8**; mp 81−82 °C. ^{1}H NMR ($CDCl_3$, 400 MHz): δ 3.36 (s, 1H, ≡H), 3.88 (s, 3H, OCH_3), 6.94−6.96 (m, 2H, Ar−H), 8.11−8.13 (m, 2H, Ar−H). MS found $(M + H)^+$ (m/z): 161.30. Calcd for $C_{10}H_8O_2$ m/z: 160.05.

*1-(2,4,6-Trimethoxyphenyl)prop-2-yn-1-one (**8b**).* Starting from 1-(2,4,6-trimethoxyphenyl)prop-2-yn-1-ol **7b**, 70% of **8b** was obtained as pale yellow solid according to the method described in above-mentioned general procedure **8**; mp 83−84 °C. ^{1}H NMR ($CDCl_3$, 400 MHz): δ 3.14 (s, 1H, ≡H), 3.76 (s, 6H, OCH_3), 3.77 (s, 3H, OCH_3), 6.03 (s, 2H, Ar−H). MS found $(M + H)^+$ (m/z): 221.20. Calcd for $C_{12}H_{12}O_4$ m/z: 220.07.

*1-(3,4,5-Trimethoxyphenyl)prop-2-yn-1-one (**8c**).* Starting from 1-(3,4,5-trimethoxyphenyl)prop-2-yn-1-ol **7c**, 70% of **8c** was obtained as pale-yellow solid according to the method described in above-mentioned general procedure **8**; mp 123−124 °C. ^{1}H NMR ($CDCl_3$, 400 MHz): δ 3.35 (s, 1H, ≡H), 3.86 (s, 3H, OCH_3), 3.88 (s, 6H, OCH_3), 7.36 (s, 2H, Ar−H). MS found $(M + H)^+$ (m/z): 221.20. Calcd for $C_{12}H_{12}O_4$ m/z: 220.07.

*1-(2-Chloro-3,4,5-trimethoxyphenyl)prop-2-yn-1-one (**8d**).* Starting from 1-(2-chloro-3,4,5-trimethoxyphenyl)prop-2-yn-1-ol **7d**, 70% of **8d** was obtained as brown solid according to the method described in above-mentioned general procedure **8**; mp 84−85 °C. ^{1}H NMR ($CDCl_3$, 400 MHz): δ 3.50 (s, 1H, ≡H), 3.91 (s, 3H, OCH_3), 3.93 (s, 3H, OCH_3), 3.99 (s, 3H, OCH_3), 7.44 (s, 1H, Ar−H). MS found $(M + H)^+$ (m/z): 255.20. Calcd for $C_{12}H_{11}ClO_4$ m/z: 254.03.

*1-(2-Bromo-3,4,5-trimethoxyphenyl)prop-2-yn-1-one (**8e**).* Starting from 1-(2-bromo-3,4,5-trimethoxyphenyl)prop-2-yn-1-ol **7e**, 70% of **8e** was obtained as brown solid according to the method described in above-mentioned general procedure **8**; mp 80−81 °C. ^{1}H NMR ($CDCl_3$, 400 MHz): δ 3.50 (s, 1H, ≡H), 3.90 (s, 3H, OCH_3), 3.93 (s, 3H, OCH_3), 3.98 (s, 3H, OCH_3), 7.47 (s, 1H, Ar−H). MS found $(M + H)^+$ (m/z): 298.90. Calcd for $C_{12}H_{11}BrO_4$ m/z: 297.98.

*1-(3,4,5-Trimethoxy-2-nitrophenyl)prop-2-yn-1-one (**8f**).* Starting from 1-(3,4,5-trimethoxy-2-nitrophenyl)prop-2-yn-1-ol **7f**, 70% of **8f** was obtained as brown solid according to the method described in above-mentioned general procedure **8**; mp 87−88 °C. ^{1}H NMR ($CDCl_3$, 400 MHz): δ 3.42 (s, 1H, ≡H), 3.88 (s, 3H, OCH_3), 3.91 (s, 3H, OCH_3), 3.93 (s, 3H, OCH_3), 7.39 (s, 1H, Ar−H). MS found $(M + H)^+$ (m/z): 266.30. Calcd for $C_{12}H_{11}NO_6$ m/z: 265.06.

*General Procedure for the Synthesis of (Z)-1-Aryl-3-arylamino-2-propen-1-one (**10**).* The ethynylketone **8** (5 mmol) was dissolved in absolute ethanol, and arylamine (5 mmol) was added. The reaction was stirred for 4 h at room temperature. After the completion of reaction (checked by TLC), the reaction mixture was diluted with water and the product filtered. The crude product was recrystallized from methanol to get pure compound **10**.

*(Z)-1-(4-Methoxyphenyl)-3-(4-methoxyphenylamino)prop-2-en-1-one (**10a**).* Starting from 1-(4-methoxyphenyl)prop-2-yn-1-one **8a** and 4-methoxyphenylamine, 76% of **10a** was obtained as yellow solid according to above-mentioned general procedure **10**; R_f = 0.71 (30% ethyl acetate in hexane); mp 187−188 °C. ^{1}H NMR ($CDCl_3$, 400 MHz): δ 3.80 (s, 3H, OCH_3), 3.86 (s, 3H, OCH_3), 5.94 (d, 1H, J = 7.8 Hz, COCH═), 6.88−6.95 (m, 4H, Ar−H), 7.02−7.05 (m, 2H, Ar−H), 7.37−7.42 (dd, 1H, J = 7.8, 12.3 Hz, ═CH-NH), 7.90−7.93 (m, 2H, Ar−H), 12.06 (d, 1H, J = 12.1 Hz, NH). MS found $(M + H)^+$ (m/z): 284.20. Calcd for $C_{17}H_{17}NO_3$ m/z: 283.12.

*(Z)-1-(4-Methoxyphenyl)-3-(3,4,5-trimethoxyphenylamino)prop-2-en-1-one (**10b**).* Starting from 1-(4-methoxyphenyl)prop-2-yn-1-one **8a** and 3,4,5-trimethoxyphenylamine, 74% of **10b** was obtained as yellow solid according to above-mentioned general procedure **10**; R_f = 0.43 (30% ethyl acetate in hexane); mp 100−101 °C. ^{1}H NMR ($CDCl_3$, 400 MHz): δ 3.82 (s, 3H, OCH_3), 3.87 (s, 9H, OCH_3), 5.98 (d, 1H, J = 12.9 Hz, COCH═), 6.31 (s, 2H, Ar−H), 6.94−6.99 (m, 2H, Ar−H), 7.39−7.44 (dd, 1H, J = 7.8, 12.3 Hz, ═CH-NH), 7.91−7.94 (m, 2H Ar−H), 12.12 (d, 1H, J = 12.0 Hz, NH). MS found $(M + H)^+$ (m/z): 344.20. Calcd for $C_{19}H_{21}NO_5$ m/z: 343.14.

*(Z)-3-(4-Methoxyphenylamino)-1-(2,4,6-trimethoxyphenyl)prop-2-en-1-one (**10c**).* Starting from 1-(2,4,6-trimethoxyphenyl)prop-2-yn-1-one **8b** and 4-methoxyphenylamine, 77% of **10c** was obtained as yellow solid according to above-mentioned general procedure **10**; R_f = 0.28 (30% ethyl acetate in hexane); mp 130−131 °C. ^{1}H NMR ($CDCl_3$, 400 MHz): δ 3.80 (s, 6H, OCH_3), 3.82 (s, 3H, OCH_3), 3.84 (s, 3H, OCH_3), 5.52 (d, 1H, J = 7.7 Hz, COCH═), 6.14 (s, 2H, Ar−H), 6.95−6.98 (m, 2H, Ar−H), 7.20−7.26 (m, 1H, ═CH-NH and 2H, Ar−H), 11.86 (d, 1H, J = 12.2 Hz, NH). MS found $(M + H)^+$ (m/z): 344.20. Calcd for $C_{19}H_{21}NO_5$ m/z: 343.14.

*(Z)-3-(2-Hydroxyphenylamino)-1-(2,4,6-trimethoxyphenyl)prop-2-en-1-one (**10d**).* Starting from 1-(2,4,6-trimethoxyphenyl)prop-2-yn-1-one **8b** and 2-aminophenol, 69% of **10d** was obtained as yellow solid according to above-mentioned general procedure **10**; R_f = 0.10 (30% ethyl acetate in hexane); mp 164−165 °C. ^{1}H NMR ($CDCl_3$, 400 MHz): δ 3.47 (s, 6H, OCH_3), 3.56 (s, 3H, OCH_3), 5.27 (d, 1H, J = 7.4 Hz, COCH═), 5.85 (s, 2H, Ar−H), 6.43−6.54 (m, 3H, Ar−H), 6.80−6.82 (m, 1H, Ar−H), 7.08−7.13 (dd, 1H, J = 7.6, 12.8 Hz, ═CH-NH), 11.85 (d, 1H, J = 12.2 Hz, NH). MS found $(M + H)^+$ (m/z): 330.20. Calcd for $C_{18}H_{19}N_2O_5$ m/z: 329.13.

*(Z)-3-(4-Chlorophenylamino)-1-(2,4,6-trimethoxyphenyl)prop-2-en-1-one (**10e**).* Starting from 1-(2,4,6-trimethoxyphenyl)prop-2-yn-1-one **8b** and 4-chlorophenylamine, 72% of **10e** was obtained as yellow solid according to above-mentioned general procedure **10**; R_f = 0.26 (30% ethyl acetate in hexane); mp 180−181 °C. ^{1}H NMR ($CDCl_3$, 400 MHz): δ 3.80 (s, 6H, OCH_3), 3.84 (s, 3H, OCH_3), 5.54 (d, 1H, J = 7.8 Hz, COCH═), 6.13 (s, 2H, Ar−H), 6.97−7.00 (m, 2H, Ar−H), 7.23−7.28 (m, 1H, ═CH-NH and 2H, Ar−H), 11.85 (d, 1H, J = 12.1 Hz, NH). MS found $(M + H)^+$ (m/z): 348.20. Calcd for $C_{18}H_{18}ClNO_4$ m/z: 347.09.

*(Z)-3-(2,4-Dimethoxyphenylamino)-1-(2,4,6-trimethoxyphenyl)-prop-2-en-1-one (**10f**).* Starting from 1-(2,4,6-trimethoxyphenyl)-prop-2-yn-1-one **8b** and 2,4-dimethoxyphenylamine, 70% of **10f** was obtained as yellow solid according to above-mentioned general

procedure **10**; R_f = 0.10 (30% ethyl acetate in hexane); mp 105−106 °C. ^{1}H NMR ($CDCl_3$, 400 MHz): δ 3.79 (s, 6H, OCH_3), 3.84 (s, 6H, OCH_3), 3.89 (s, 3H, OCH_3), 5.47 (d, 1H, J = 7.6 Hz, COCH═), 6.12 (s, 2H, Ar−H), 6.44−6.50 (m, 2H, Ar−H), 7.03 (d, 1H, J = 8.6 Hz, Ar−H), 7.27−7.33 (dd, 1H, J = 7.6, 12.8 Hz, ═CH-NH), 11.90 (d, 1H, J = 12.1 Hz, NH). MS found $(M + H)^+$ (m/z): 374.30. Calcd for $C_{20}H_{23}NO_6$ m/z: 373.15.

*(Z)-1-(2,4,6-Trimethoxyphenyl)-3-(2,4,6-trimethoxyphenylamino)prop-2-en-1-one (**10g**).* Starting from 1-(2,4,6-trimethoxyphenyl)prop-2-yn-1-one **8b** and 2,4,6-trimethoxyphenylamine, 80% of **10g** was obtained as yellow solid according to above-mentioned general procedure **10**; R_f = 0.06 (30% ethyl acetate in hexane); mp 129−130 °C. ^{1}H NMR ($CDCl_3$, 400 MHz): δ 3.78 (s, 6H, OCH_3), 3.80 (s, 3H, OCH_3), 3.82 (s, 3H, OCH_3), 3.86 (s, 6H, OCH_3), 5.35 (d, 1H, J = 7.5 Hz, COCH═), 6.12 (s, 2H, Ar−H), 6.17 (s, 2H, Ar−H), 7.85−7.90 (dd, 1H, J = 7.5, 12.7 Hz, ═CH-NH), 12.00 (d, 1H, J = 12.2 Hz, NH). MS found $(M + H)^+$ (m/z): 404.20. Calcd for $C_{21}H_{25}NO_7$ m/z: 403.16.

*(Z)-1-(2,4,6-Trimethoxyphenyl)-3-(3,4,5-trimethoxyphenylamino)prop-2-en-1-one (**10h**).* Starting from 1-(2,4,6-trimethoxyphenyl)prop-2-yn-1-one **8b** and 3,4,5-trimethoxyphenylamine, 75% of **10h** was obtained as yellow solid according to above-mentioned general procedure **10**; R_f = 0.08 (30% ethyl acetate in hexane); mp 177−178 °C. ^{1}H NMR ($CDCl_3$, 300 MHz): δ 3.82−3.90 (m, 18H, OCH_3), 5.55 (d, 1H, J = 7.6 Hz, COCH═), 6.19 (s, 2H, Ar−H), 6.40 (s, 2H, Ar−H), 7.30−7.37 (dd, 1H, J = 7.6, 12.8 Hz, ═CH-NH), 11.98 (d, 1H, J = 12.3 Hz, NH). MS found $(M + H)^+$ (m/z): 404.20. Calcd for $C_{21}H_{25}NO_7$ m/z: 403.16.

*(Z)-3-(2-Hydroxyphenylamino)-1-(3,4,5-trimethoxyphenyl)prop-2-en-1-one (**10i**).* Starting from 1-(3,4,5-trimethoxyphenyl)prop-2-yn-1-one **8c** and 2-aminophenol, 72% of **10i** was obtained as yellow solid according to above-mentioned general procedure **10**; R_f = 0.22 (30% ethyl acetate in hexane); mp 190−191 °C. ^{1}H NMR ($CDCl_3$, 400 MHz): δ 3.89 (s, 3H, OCH_3), 3.93 (s, 6H, OCH_3), 6.02 (d, 1H, J = 7.7 Hz, COCH═), 6.91 (s, 2H, Ar−H), 7.18−7.26 (m, 4H, Ar−H), 7.57−7.62 (dd, 1H, J = 7.7, 12.8 Hz, ═CH-NH), 12.35 (d, 1H, J = 12.4 Hz, NH). MS found $(M + H)^+$ (m/z): 330.20. Calcd for $C_{18}H_{19}N_2O_5$ m/z: 329.13.

*(Z)-3-(3-Hydroxyyphenylamino)-1-(3,4,5-trimethoxyphenyl)prop-2-en-1-one (**10j**).* Starting from 1-(3,4,5-trimethoxyphenyl)prop-2-yn-1-one **8c** and 3-aminophenol, 70% of **10j** was obtained as yellow solid according to above-mentioned general procedure **10**; R_f = 0.64 (50% ethyl acetate in hexane); mp 120−121 °C. ^{1}H NMR ($CDCl_3$, 400 MHz): δ 3.74 (s, 3H, OCH_3), 3.76 (s, 6H, OCH_3), 5.36 (s, 1H, OH), 5.80 (d, 1H, J = 7.8 Hz, COCH═), 6.38−6.51 (m, 3H, Ar−H), 7.01−7.05 (m, 3H, Ar−H), 7.28−7.33 (dd, 1H, J = 8.0, 12.3 Hz, ═CH-NH), 11.88 (d, 1H, J = 12.3 Hz, NH). MS found $(M + H)^+$ (m/z): 330.10. Calcd for $C_{18}H_{19}NO_5$ m/z: 329.13.

*(Z)-3-(2-Methoxyphenylamino)-1-(3,4,5-trimethoxyphenyl)prop-2-en-1-one (**10k**).* Starting from 1-(3,4,5-trimethoxyphenyl)prop-2-yn-1-one **8c** and 2-methoxyphenylamine, 81% of **10k** was obtained as yellow solid according to above-mentioned general procedure **10**; R_f = 0.46 (30% ethyl acetate in hexane); mp 118−119 °C. ^{1}H NMR ($CDCl_3$, 400 MHz): δ 3.84 (s, 3H, OCH_3), 3.86 (s, 6H, OCH_3), 3.91 (s, 3H, OCH_3), 5.94 (d, 1H, J = 7.8 Hz, COCH═), 6.85−6.97 (m, 4H, Ar−H), 7.16 (s, 2H, Ar−H), 7.44−7.49 (dd, 1H, J = 7.6, 12.6 Hz, ═CH-NH), 12.10 (d, 1H, J = 12.1 Hz, NH). MS found $(M + H)^+$ (m/z): 344.20. Calcd for $C_{19}H_{21}NO_5$ m/z: 343.14.

*(Z)-3-(4-Methoxyphenylamino)-1-(3,4,5-trimethoxyphenyl)prop-2-en-1-one (**10l**).* Starting from 1-(3,4,5-trimethoxyphenyl)prop-2-yn-1-one **8c** and 4-methoxyaniline, 82% of **10l** was obtained as yellow solid according to above-mentioned general procedure **10**; R_f = 0.40 (30% ethyl acetate in hexane); mp 107−108 °C. ^{1}H NMR ($CDCl_3$, 300 MHz): δ 3.81 (s, 3H, OCH_3), 3.91 (s, 3H, OCH_3), 3.94 (s, 6H, OCH_3), 5.93 (d, 1H, J = 7.8 Hz, COCH═), 6.89−6.92 (m, 2H, Ar−H), 7.04−7.07 (m, 2H, Ar−H), 7.20 (s, 2H, Ar−H), 7.41−7.48 (dd, 1H, J = 7.8, 12.3 Hz, ═CH-NH), 12.18 (d, 1H, J = 12.3 Hz, NH). MS found $(M + H)^+$ (m/z): 344.20. Calcd for $C_{19}H_{21}NO_5$ m/z: 343.14.

*(Z)-3-(4-Chlorophenylamino)-1-(3,4,5-trimethoxyphenyl)prop-2-en-1-one (**10m**).* Starting from 1-(3,4,5-trimethoxyphenyl)prop-2-yn-1-one **8c** and 4-chlorophenylamine, 72% of **10m** was obtained as yellow solid according to above-mentioned general procedure **10**; R_f = 0.80 (50% ethyl acetate in hexane); mp 147−148 °C. ^{1}H NMR ($CDCl_3$, 300 MHz): δ 3.92 (s, 3H, OCH_3), 3.94 (s, 6H, OCH_3), 6.01 (d, 1H, J = 8.1 Hz, COCH═), 7.02−7.05 (m, 2H, Ar−H), 7.20 (s, 2H, Ar−H), 7.30−7.33 (m, 2H, Ar−H), 7.42−7.49 (dd, 1H, J = 7.8, 12.3 Hz, ═CH-NH), 12.13 (d, 1H, J = 12.3 Hz, NH). MS found $(M + H)^+$ (m/z): 348.10. Calcd for $C_{18}H_{18}ClNO_4$ m/z: 347.09.

*(Z)-3-(4-Trifluoromethoxyphenylamino)-1-(3,4,5-trimethoxyphenyl)prop-2-en-1-one (**10n**).* Starting from 1-(3,4,5-trimethoxyphenyl)prop-2-yn-1-one **8c** and 4-trifluoromethoxyphenylamine, 75% of **10n** was obtained as yellow solid according to above-mentioned general procedure **10**; R_f = 0.80 (50% ethyl acetate in hexane); mp 107−108 °C. ^{1}H NMR ($CDCl_3$, 300 MHz): δ 3.92 (s, 3H, OCH_3), 3.94 (s, 6H, OCH_3), 6.02 (d, 1H, J = 7.8 Hz, COCH═), 7.08−7.12 (m, 2H, Ar−H), 7.20−7.24 (m, 4H, Ar−H), 7.42−7.47 (dd, 1H, J = 8.1, 12.3 Hz, ═CH-NH), 12.15 (d, 1H, J = 12.0 Hz, NH). MS found $(M + H)^+$ (m/z): 398.10. Calcd for $C_{19}H_{18}F_3NO_5$ m/z: 397.11.

*(Z)-3-(4-Trifluoromethylphenylamino)-1-(3,4,5-trimethoxyphenyl)prop-2-en-1-one (**10o**).* Starting from 1-(3,4,5-trimethoxyphenyl)prop-2-yn-1-one **8c** and 4-trifluoromethylphenylamine, 68% of **10o** was obtained as yellow solid according to above-mentioned general procedure **10**; R_f = 0.80 (50% ethyl acetate in hexane); mp 92−93 °C. ^{1}H NMR ($CDCl_3$, 400 MHz): δ 3.86 (s, 3H, OCH_3), 3.87 (s, 6H, OCH_3), 6.01 (d, 1H, J = 8.0 Hz, COCH═), 7.10 (d, 2H, J = 8.4 Hz, Ar−H), 7.15 (s, 2H, Ar−H), 7.43−7.48 (dd, 1H, J = 8.0, 12.0 Hz, ═CH-NH), 7.58 (d, 2H, J = 8.5 Hz, Ar−H), 12.05 (d, 1H, J = 12.3 Hz, NH). MS found $(M + H)^+$ (m/z): 382.20. Calcd for $C_{19}H_{18}F_3NO_4$ m/z: 381.12.

*(Z)-3-(3-Hydroxy-4-methoxyphenylamino)-1-(3,4,5-trimethoxyphenyl)prop-2-en-1-one (**10p**).* Starting from 1-(3,4,5-trimethoxyphenyl)prop-2-yn-1-one **8c** and 2-methoxy-5-aminophenol, 70% of **10p** was obtained as yellow solid according to above-mentioned general procedure **10**; R_f = 0.26 (30% ethyl acetate in hexane); mp 142−143 °C. ^{1}H NMR ($CDCl_3$, 400 MHz): δ 3.59 (s, 3H, OCH_3), 3.62 (s, 3H, OCH_3), 3.65 (s, 6H, OCH_3), 5.64 (d, 1H, J = 7.7 Hz, COCH═), 6.28−6.31(m, 1H, Ar−H), 6.46 (d, 1H, J = 2.6 Hz, Ar−H), 6.53 (d, 1H, J = 8.6 Hz, Ar−H), 6.91 (s, 2H, Ar−H), 7.10−7.15 (dd, 1H, J = 7.7, 12.3 Hz, ═CH-NH), 11.80 (d, 1H, J = 12.1 Hz, NH). MS found $(M + H)^+$ (m/z): 360.10. Calcd for $C_{19}H_{21}NO_6$ m/z: 359.14.

*Synthesis of (Z)-3-(3-Amino-4-methoxyphenylamino)-1-(3,4,5-trimethoxyphenyl)-prop-2-en-1-one (**10q**). . Step 1: Synthesis of (Z)-3-(4-nitro-3-methoxyphenylamino)-1-(3,4,5-trimethoxyphenyl)-prop-2-en-1-one.* The ethynylketone **8c** (1.94 g, 5 mmol) was dissolved in absolute ethanol, and 4-methoxy-3-nitrophenylamine (0.84 g, 5 mmol) was added. The reaction was stirred for 4 h at room temperature. After the completion of reaction by TLC, the reaction mixture was diluted with water and filtered the product. The crude product was recrystallized from methanol to get pure compound with 74% yield as yellow solid, R_f = 0.40 (30% ethyl acetate in hexane); mp 115−116 °C. ^{1}H NMR ($CDCl_3$, 300 MHz): δ 3.93 (s, 3H, OCH_3), 3.96 (s, 3H, OCH_3), 3.98 (s, 6H, OCH_3), 6.05 (d, 1H, J = 7.8 Hz, COCH═), 7.13 (d, 1H, J = 9 Hz, Ar−H), 7.21 (s, 2H, Ar−H), 7.28−7.30 (m, 2H, Ar−H), 7.42−7.46 (dd, 1H, J = 7.8, 12.6 Hz, ═CH-NH), 12.22 (d, 1H, J = 11.7 Hz, NH). MS found $(M + H)^+$ (m/z): 389.20. Calcd for $C_{19}H_{20}N_2O_7$ m/z: 388.13.

*Step 2: Synthesis of (Z)-3-(3-Amino-4-methoxyphenylamino)-1-(3,4,5-trimethoxyphenyl)-prop-2-en-1-one (**10q**).* The above nitro compound (2.0 g, 5.11 mmol) obtained from step 1 was dissolved in acetone/water (2:1 ratio) 100 mL and heated to 50 °C for 30 min. After completion of the reaction by TLC, the contents were cooled to room temperature and the reaction mixture was extracted with ethyl acetate. The organic extract was washed with water and brine solution and dried over anhydrous Na_2SO_4 and concentrated under vacuum to get crude product. The pure product **10q** was obtained by flash chromatography, R_f = 0.22 (30% ethyl acetate in hexane). Yield: 69%; yellow solid; mp 98−99 °C. ^{1}H NMR ($CDCl_3$, 400 MHz): δ 3.65 (s, 3H, OCH_3), 3.72 (s, 3H, OCH_3), 3.73−3.79 (m, 6H, OCH_3 and 2H,

dx.doi.org/10.1021/jm300176j | J. Med. Chem. 2012, 55, 5174−5187

NH_2), 5.70 (d, 1H, J = 7.7 Hz, COCH═), 6.25−6.30 (m, 2H, Ar−H), 6.55 (d, 1H, J = 8.4 Hz, Ar−H), 7.00 (s, 2H, Ar−H), 7.19−7.24 (dd, 1H, J = 7.7, 12.5 Hz, ═CH-NH), (d, 1H, J = 12.0 Hz, NH). MS found $(M + H)^+$ (m/z): 359.20. Calcd for $C_{19}H_{22}N_2O_5$ m/z: 358.15.

(Z)-3-(3-Fluoro-4-methoxyphenylamino)-1-(3,4,5-trimethoxyphenyl)prop-2-en-1-one (**10r**). Starting from 1-(3,4,5-trimethoxyphenyl)prop-2-yn-1-one **8c** and 3-fluoro-4-methoxyaniline, 68% of **10r** was obtained as yellow solid according to above-mentioned general procedure **10**; R_f = 0.40 (30% ethyl acetate in hexane); mp 110−111 °C. ^{1}H NMR ($CDCl_3$, 400 MHz): δ 4.05 (s, 3H, OCH_3), 4.08 (s, 3H, OCH_3), 4.10 (s, 6H, OCH_3), 6.13 (d, 1H, J = 7.8 Hz, COCH═), 6.98−7.14 (m, 3H, Ar−H), 7.36 (s, 2H, Ar−H), 7.51−7.56 (dd, 1H, J = 7.8, 12.2 Hz, ═CH-NH), 12.0 (d, 1H, J = 12.1 Hz, NH). MS found $(M + H)^+$ (m/z): 362.20. Calcd for $C_{19}H_{20}FNO_5$ m/z: 361.13.

(Z)-3-(3-Chloro-4-methoxyphenylamino)-1-(3,4,5-trimethoxyphenyl)prop-2-en-1-one (**10s**). Starting from 1-(3,4,5-trimethoxyphenyl)prop-2-yn-1-one **8c** and 3-chloro-4-methoxyphenylamine, 70% of **10s** was obtained as yellow solid according to above-mentioned general procedure **10**; R_f = 0.66 (50% ethyl acetate in hexane); mp 133−134 °C. ^{1}H NMR ($CDCl_3$, 300 MHz): δ 3.90 (s, 3H, OCH_3), 3.91 (s, 3H, OCH_3), 3.94 (s, 6H, OCH_3), 5.96 (d, 1H, J = 7.8 Hz, COCH═), 6.90−6.99 (m, 2H, Ar−H), 7.17 (d, 1H, J = 2.5 Hz, Ar−H), 7.19 (s, 2H, Ar−H), 7.35−7.42 (dd, 1H, J = 7.6, 12.6 Hz, ═CH-NH), 12.15 (d, 1H, J = 12.3 Hz, NH). MS found $(M + H)^+$ (m/z): 378.20. Calcd for $C_{19}H_{20}ClNO_5$ m/z: 377.10.

(Z)-3-(2-Chloro-5-hydroxyphenylamino)-1-(3,4,5-trimethoxyphenyl)prop-2-en-1-one (**10t**). Starting from 1-(3,4,5-trimethoxyphenyl)prop-2-yn-1-one **8c** and 3-amino-4-chlorophenol, 73% of **10t** was obtained as yellow solid according to above-mentioned general procedure **10**; R_f = 0.56 (50% ethyl acetate in hexane); mp 99−100 °C. ^{1}H NMR ($CDCl_3$, 300 MHz): δ 3.87 (s, 3H, OCH_3), 3.88 (s, 6H, OCH_3), 6.02 (d, 1H, J = 8.0 Hz, COCH═), 6.40−6.42 (m, 1H, Ar−H), 6.67 (d, 1H, J = 2.1 Hz, Ar−H), 7.16 (s, 2H, Ar−H), 7.34−7.36 (m, 1H, ═CH-NH and 1H, Ar−H), 12.20 (d, 1H, J = 12.2 Hz, NH). MS found $(M + H)^+$ (m/z): 364.10. Calcd for $C_{18}H_{18}ClNO_5$ m/z: 363.09.

(Z)-1-(3,4,5-Trimethoxyphenyl)-3-(2,4,6-trimethoxyphenylamino)prop-2-en-1-one (**10u**). Starting from 1-(3,4,5-trimethoxyphenyl)prop-2-yn-1-one **8c** and 2,4,6-trimethoxyphenylamine, 80% of **10u** was obtained as yellow solid according to above-mentioned general procedure **10**; R_f = 0.20 (30% ethyl acetate in hexane); mp 132−133 °C. ^{1}H NMR ($CDCl_3$, 400 MHz): δ 3.78 (s, 3H, OCH_3), 3.86 (s, 6H, OCH_3), 3.87 (s, 3H, OCH_3), 3.89 (s, 6H, OCH_3), 5.81 (d, 1H, J = 7.7 Hz, COCH═), 6.16 (s, 2H, Ar−H), 7.17 (s, 2H, Ar−H), 7.89−7.94 (dd, 1H, J = 7.6, 12.7 Hz, ═CH-NH), 12.05 (d, 1H, J = 12.1 Hz, NH). MS found $(M + H)^+$ (m/z): 404.10. Calcd for $C_{21}H_{25}NO_7$ m/z: 403.16.

(Z)-1-(3,4,5-Trimethoxyphenyl)-3-(3,4,5-trimethoxyphenylamino)prop-2-en-1-one (**10v**). Starting from 1-(3,4,5-trimethoxyphenyl)prop-2-yn-1-one **8c** and 3,4,5-trimethoxyphenylamine, 78% of **10v** was obtained as yellow solid according to above-mentioned general procedure **10**; R_f = 0.22 (30% ethyl acetate in hexane); mp 181−182 °C. ^{1}H NMR ($CDCl_3$, 400 MHz): δ 3.75 (s, 3H, OCH_3), 3.80 (s, 6H, OCH_3), 3.84 (s, 3H, OCH_3), 3.87 (s, 6H, OCH_3), 5.90 (d, 1H, J = 7.8 Hz, COCH═), 6.25 (s, 2H, Ar−H), 7.13 (s, 2H, Ar−H), 7.36−7.41 (dd, 1H, J = 7.8, 12.2 Hz, ═CH-NH), 12.20 (d, 1H, J = 12.2 Hz, NH). MS found $(M + H)^+$ (m/z): 404.20. Calcd for $C_{21}H_{25}NO_7$ m/z: 403.16.

(Z)-3-(1H-Indole-5-ylamino)-1-(3,4,5-trimethoxyphenyl)prop-2-en-1-one (**10w**). Starting from 1-(3,4,5-trimethoxyphenyl)prop-2-yn-1-one **8c** and 5-aminoindole, 65% of **10w** was obtained as yellow solid according to above-mentioned general procedure **10**; R_f = 0.24 (30% ethyl acetate in hexane); mp 174−175 °C. ^{1}H NMR ($CDCl_3$, 400 MHz): δ 3.98 (s, 3H, OCH_3), 4.01 (s, 6H, OCH_3), 6.01 (d, 1H, J = 7.6 Hz, COCH═), 6.60 (s, 1H, Ar−H), 7.07 (d, 1H, J = 6.7 Hz, Ar−H), 7.29−7.45 (m, 5H, Ar−H), 7.62−7.67 (dd, 1H, J = 7.6, 12.8 Hz, ═CH-NH), 8.29 (bs, 1H, NH), 12.38 (d, 1H, J = 12.1 Hz, NH). MS found $(M + H)^+$ (m/z): 353.20. Calcd for $C_{20}H_{20}N_2O_4$ m/z: 352.14.

(Z)-3-(1H-Indole-6-ylamino)-1-(3,4,5-trimethoxyphenyl)prop-2-en-1-one (**10x**). Starting from 1-(3,4,5-trimethoxyphenyl)prop-2-yn-1-one **8c** and 6-aminoindole, 69% of **10x** was obtained as yellow solid according to above-mentioned general procedure **10**; R_f = 0.60 (30% ethyl acetate in hexane); mp 131−132 °C. ^{1}H NMR ($CDCl_3$, 300 MHz): δ 3.86 (s, 3H, OCH_3), 3.88 (s, 6H, OCH_3), 6.07 (d, 1H, J = 8.1 Hz COCH═), 7.16 (s, 2H, Ar−H), 7.19 (s, 1H, Ar−H), 7.48−7.60 (m, 1H, ═CH-NH and 1H, Ar−H), 7.68−7.71 (m, 2H, Ar−H), 8.00 (d, 1H, J = 8.4 Hz, Ar−H), 8.72 (brs, 1H, NH), 12.26 (d, 1H, J = 12.3 Hz, NH). MS found $(M + H)^+$ (m/z): 353.20. Calcd for $C_{20}H_{20}N_2O_4$ m/z: 352.14.

(Z)-3-(1H-Indole-7-ylamino)-1-(3,4,5-trimethoxyphenyl)prop-2-en-1-one (**10y**). Starting from 1-(3,4,5-trimethoxyphenyl)prop-2-yn-1-one **8c** and 7-aminoindole, 66% of **10y** was obtained as yellow solid according to above-mentioned general procedure **10**; R_f = 0.82 (50% ethyl acetate in hexane); mp 86−87 °C. ^{1}H NMR ($CDCl_3$, 400 MHz): δ 3.86 (s, 3H, OCH_3), 3.87 (s, 6H, OCH_3), 6.01 (d, 1H, J = 7.4 Hz, COCH═), 6.55 (s, 1H, Ar−H), 6.96−7.09 (m, 3H, Ar−H), 7.15 (s, 2H, Ar−H), 7.40 (d, 1H, J = 7.6 Hz, Ar−H), 7.57−7.62 (dd, 1H, J = 7.8, 12.3 Hz, ═CH-NH), 8.75 (s, 1H, NH), 12.45 (d, 1H, J = 12.3 Hz, NH). MS found $(M + H)^+$ (m/z): 353.30. Calcd for $C_{20}H_{20}N_2O_4$ m/z: 352.14.

(Z)-3-(1H-Indazole-5-ylamino)-1-(3,4,5-trimethoxyphenyl)prop-2-en-1-one (**10z**). Starting from 1-(3,4,5-trimethoxyphenyl)prop-2-yn-1-one **8c** and 4-aminoindazole, 65% of **10z** was obtained as yellow solid according to above-mentioned general procedure **10**; R_f = 0.16 (50% ethyl acetate in hexane); mp 160−161 °C. ^{1}H NMR ($CDCl_3$, 300 MHz): δ 3.92 (s, 3H, OCH_3), 3.95 (s, 6H, OCH_3), 6.00 (d, 1H, J = 7.8 Hz, COCH═), 7.20 (s, 2H, Ar−H), 7.46−7.60 (m, 1H, ═CH and 4H, Ar−H), 8.06 (s, 1H, NH), 12.31 (d, 1H, J = 12.3 Hz, NH). MS found $(M + H)^+$ (m/z): 354.20. Calcd for $C_{19}H_{19}N_3O_4$ m/z: 353.14.

(Z)-3-(Quinolin-3-ylamino)-1-(3,4,5-trimethoxyphenyl)prop-2-en-1-one (**10aa**). Starting from 1-(3,4,5-trimethoxyphenyl)prop-2-yn-1-one **8c** and 3-aminoquinoline, 64% of **10aa** was obtained as yellow solid according to above-mentioned general procedure **10**; R_f = 0.36 (50% ethyl acetate in hexane); mp 120−121 °C. ^{1}H NMR ($CDCl_3$, 300 MHz): δ 3.92 (s, 3H, OCH_3), 3.95 (s, 6H, OCH_3), 5.96 (d, 1H, J = 7.8 Hz, COCH═), 6.52−6.54 (m, 1H, Ar−H), 6.94−6.97 (m, 1H, Ar−H), 7.13 (brs, 1H, Ar−H), 7.17−7.19 (m, 1H, Ar−H), 7.22 (s, 2H, Ar−H), 7.55−7.62 (m, 1H, ═CH-NH and 1H, Ar−H), 8.26 (brs, 1H, Ar−H), 12.35 (d, 1H, J = 12.3 Hz, NH). MS found $(M + H)^+$ (m/z): 365.10. Calcd for $C_{21}H_{20}N_2O_4$ m/z: 364.14.

(Z)-3-(2-Methyl-1H-indole-5-ylamino)-1-(3,4,5-trimethoxyphenyl)prop-2-en-1-one (**10ab**). Starting from 1-(3,4,5-trimethoxyphenyl)prop-2-yn-1-one **8c** and 5-amino-2-methylindole, 65% of **10ab** was obtained as yellow solid according to above-mentioned general procedure **10**; R_f = 0.56 (50% ethyl acetate in hexane); mp 176−177 °C. ^{1}H NMR ($CDCl_3$, 400 MHz): δ 2.39 (s, 3H, CH_3), 3.85 (s, 3H, OCH_3), 3.88 (s, 6H, OCH_3), 5.86 (d, 1H, J = 7.6 Hz, COCH═), 6.13 (s, 1H, Ar−H), 6.83−6.85 (m, 1H, Ar−H), 7.16 (s, 2H, Ar−H), 7.17−7.20 (m, 2H, Ar−H), 7.48−7.53 (dd, 1H, J = 7.6, 12.5 Hz, ═CH-NH), 7.87 (s, 1H, NH), 12.25 (d, 1H, J = 12.3 Hz, NH). MS found $(M + H)^+$ (m/z): 367.20. Calcd for $C_{21}H_{22}N_2O_4$ m/z: 366.16.

(Z)-1-(2-Bromo-3,4,5-trimethoxyphenyl)-3-(2-hydroxyphenylamino)prop-2-en-1-one (**10ac**). Starting from 1-(2-bromo-3,4,5-trimethoxyphenyl)prop-2-yn-1-one **8e** and 2-amino-phenol, 70% of **10ac** was obtained as yellow solid according to above-mentioned general procedure **10**; R_f = 0.66 (50% ethyl acetate in hexane); mp 189−190 °C. ^{1}H NMR ($CDCl_3$, 300 MHz): δ 3.85 (s, 3H, OCH_3), 3.94 (s, 3H, OCH_3), 3.95 (s, 3H, OCH_3), 5.77 (d, 1H, J = 7.5 Hz, COCH═), 6.78−6.80 (m, 1H, Ar−H), 6.87−6.90 (m, 2H, Ar−H), 6.94 (s, 1H, Ar−H), 7.17−7.20 (m, 1H, Ar−H), 7.56−7.63 (dd, 1H, J = 7.8, 13.2 Hz, ═CH-NH), 12.33 (d, 1H, J = 13.2 Hz, NH). MS found $(M + H)^+$ (m/z): 408.10. Calcd for $C_{18}H_{18}BrNO_5$ m/z: 407.04.

(Z)-1-(2-Bromo-3,4,5-trimethoxyphenyl)-3-(4-methoxyphenylamino)prop-2-en-1-one (**10ad**). Starting from 1-(2-bromo-3,4,5-trimethoxyphenyl)prop-2-yn-1-one **8e** and 4-methoxy-

dx.doi.org/10.1021/jm300176j | J. Med. Chem. 2012, 55, 5174−5187

phenylamine, 68% of **10ad** was obtained as yellow solid according to above-mentioned general procedure **10**; R_f = 0.74 (50% ethyl acetate in hexane); mp 70−71 °C. ^{1}H NMR ($CDCl_3$, 300 MHz): δ 3.81 (s, 3H, OCH_3), 3.88 (s, 3H, OCH_3), 3.91 (s, 3H, OCH_3), 3.92 (s, 3H, OCH_3), 5.63 (d, 1H, J = 7.5 Hz, COCH═), 6.86 (s, 1H, Ar−H), 6.89−6.93 (m, 2H, Ar−H), 7.05−7.09 (m, 2H, Ar−H), 7.37−7.44 (dd, 1H, J = 7.5, 12.6 Hz, ═CH-NH), 11.94 (d, 1H, J = 12.6 Hz, NH). MS found $(M + H)^+$ (m/z): 424.10. Calcd for $C_{19}H_{20}BrNO_5$ m/z: 421.05.

*(Z)1-(2-Bromo-3,4,5-trimethoxyphenyl)-3-(3-hydroxy-4-methoxyphenylamino)-prop-2-en-1-one (**10ae**).* Starting from 1-(2-bromo-3,4,5-trimethoxyphenyl)prop-2-yn-1-one **8e** and 2-methoxy-5-aminophenol, 65% of **10ae** was obtained as yellow solid according to above-mentioned general procedure **10**; R_f = 0.60 (50% ethyl acetate in hexane); mp 150−151 °C. ^{1}H NMR ($CDCl_3$, 300 MHz): δ 3.81 (s, 3H, OCH_3), 3.89 (s, 3H, OCH_3), 3.91 (s, H, OCH_3), 3.92 (3H, OCH_3) 5.64 (d, 1H, J = 7.5 Hz, COCH═), 5.73 (brs, 1H, OH), 6.58−6.62 (m, 1H, Ar−H), 6.76−6.84 (m, 2H, Ar−H), 6.86 (s, 1H, Ar−H), 7.34−7.41 (dd, 1H, J = 7.5, 12.6 Hz, ═CH-NH), 11.86 (d, 1H, J = 12.3 Hz, NH). MS found $(M + H)^+$ (m/z): 438.10. Calcd for $C_{19}H_{20}BrNO_6$ m/z: 437.05.

*(Z)-1-(2-Bromo-3,4,5-trimethoxyphenyl)-3-(1H-indol-5-ylamino)-prop-2-en-1-one (**10af**).* Starting from 1-(2-bromo-3,4,5-trimethoxyphenyl)prop-2-yn-1-one **8e** and 5-aminoindole, 64% of **10af** was obtained as yellow solid according to above-mentioned general procedure **10**; R_f = 0.70 (50% ethyl acetate in hexane); mp 109−110 °C. ^{1}H NMR ($CDCl_3$, 300 MHz): δ 3.78 (s, 3H, OCH_3), 3.83 (s, 6H, OCH_3), 5.54 (d, 1H, J = 7.5 Hz, COCH═), 6.42 (s, 1H, Ar−H), 6.80 (s, 1H, Ar−H), 6.87−7.91 (m, 1H, Ar−H), 7.13−7.18 (m, 1H, Ar−H), 7.25−7.30 (m, 2H, Ar−H), 7.42−7.49 (dd, 1H, J = 7.6, 12.7 Hz, ═CH-NH), 8.50 (s, 1H, NH), 12.00 (d, 1H, J = 12.6 Hz, NH). MS found $(M + H)^+$ (m/z): 431.10. Calcd for $C_{20}H_{19}BrN_2O_4$ m/z: 430.05.

*(Z)-1-(2-Chloro-3,4,5-trimethoxyphenyl)-3-(3-hydroxy-4-methoxyphenylamino)prop-2-en-1-one (**10ag**).* Starting from 1-(2-chloro-3,4,5-trimethoxyphenyl)prop-2-yn-1-one **8d** and 2-methoxy-5-aminophenol, 65% of **10ag** was obtained as yellow solid according to above-mentioned general procedure **10**; R_f = 0.60 (50% ethyl acetate in hexane); mp 102−103 °C. ^{1}H NMR ($CDCl_3$, 300 MHz): δ 3.89 (s, 3H, OCH_3), 3.90 (s, 3H, OCH_3), 3.93 (s, 3H, OCH_3), 3.94 (s, 3H, OCH_3) 5.73 (d, 1H, J = 7.5 Hz, COCH═), 5.76 (brs, 1H, OH), 6.59−6.63 (m, 1H, Ar−H), 6.76−6.85 (m, 2H, Ar−H), 6.86 (s, 1H, Ar−H), 7.35−7.42 (dd, 1H, J = 7.5, 12.6 Hz, ═CH-NH), 11.93 (d, 1H, J = 12.3 Hz, NH). MS found $(M + H)^+$ (m/z): 394.20. Calcd for $C_{19}H_{20}ClNO_6$ m/z: 393.10.

*(Z)-3-(4-Methoxyphenylamino)-1-(3,4,5-trimethoxy-2-nitrophenyl)prop-2-en-1-one (**10ah**).* Starting from 1-(3,4,5-trimethoxy-2-nitrophenyl)prop-2-yn-1-one **8f** and 4-methoxyphenylamine 60% of **10ah** was obtained as yellow solid according to above-mentioned general procedure **10**; R_f = 0.68 (50% ethyl acetate in hexane); mp 132−133 °C. ^{1}H NMR ($CDCl_3$, 300 MHz): δ 3.82 (s, 3H, OCH_3), 3.96 (s, 6H, OCH_3), 4.00 (s, 3H, OCH_3), 5.63 (d, 1H, J = 7.5 Hz, COCH═), 6.89−6.92 (m, 2H, Ar−H), 6.97 (s, 1H, Ar−H), 7.04−7.07 (m, 2H, Ar−H), 7.39−7.45 (dd, 1H, J = 7.5, 12.6 Hz, ═CH-NH), 11.93 (d, 1H, J = 12.9 Hz, NH). MS found $(M + H)^+$ (m/z): 389.10. Calcd for $C_{19}H_{20}N_2O_7$ m/z: 388.13.

Biology. *Tissue Culture and Reagents.* Paclitaxel was purchased from Sigma. Cell lines were purchased from ATCC. Cell lines were routinely grown in DMEM or RPM1 (CellGro) supplemented with 10% fetal bovine serum (CellGeneration, CO) and 1 unit/mL penicillin−streptomycin (Gibco).

Cytotoxicity Assay. We have tested a number of tumor cell lines using a dose response end point assay system. The cells were grown in either DMEM or RPMI supplemented with 10% fetal bovine serum and 1unit/mL penicillin−streptomycin solution. The tumor cells were plated into six well dishes at a cell density of 1.0×10^5 cells/mL/well, and compounds were added 24 h later at various concentrations. Cell counts were determined from duplicate wells after 96 h of treatment. The total number of viable cells was determined by trypan blue exclusion.

Flow Cytometry. Cancer cell line DU145 (human prostate tumor) cells, were grown in DMEM (Cellgro) supplemented with 10% fetal bovine serum and 1 unit/mL penicillin−streptomycin. The cells were plated onto 100 mm^2 dishes at a cell density of 1.0×10^6 cells/dish, and 24 h later, they were treated with 2.5 μM of the compound. The cells were harvested 24, 48, and 72 h after treatment. The cells were removed from the plate by trypsin digestion and combined with the nonattached cells found in the medium. The cell pellets were washed in phosphate buffered saline (PBS) and fixed in ice cold 70% ethanol for at least 24 h. The fixed cells were then washed with room temperature PBS and stained with propidium iodide (50 mg/mL) and RNase A (0.5 mg) for 30 min at 37 °C. The stained cells were then analyzed on a Becton-Dickinson (BD) (FACScan) flow cytometer and the data analyzed by cell cycle analysis software (Modfit, BD).

Western Blotting Analysis. HeLa cells were harvested at the indicated times, and cell pellets were frozen on dry ice before lysis. Cell pellets were lysed (25 mM HEPES, 0.1% Triton-X100, 300 mM NaCl, 20 mM β-glycerophosphate, 0.5 mM DTT, 1.0 mM EDTA, 1.5 mM $MgCl_2$, pH 7.5, 0.2 mM sodium orthovanadate, and protease inhibitors). Then 100 μg of each lysate was resolved by 10%-SDS-polyacrylamide gel electrophoresis. The resolved proteins were transferred onto nitrocellulose filter paper and hybridized to the following antibodies: phosphospecific histone H3 (Upstate, cat. 05−806), histone H3 (upstate, cat. 07−690), bcl-2 (BD Biosciences, cat. 610558), bub R1 (BD Biosciences, cat. 612503), plk-1(Santa Cruz, sc-17783), cyclin B1(Santa Cruz, sc-594), PARP (BD Biosciences, cat. 556362), and GAPDH (Fitzgerald, cat. RDI-TRK5G4−6C5). Following the primary hybridization, the blots were then treated with secondary antibodies conjugated to infrared dyes (IRDye 800 or IRDye 680) and analyzed on an infrared scanning system (Odyssey, Li-Cor Biosciences, NE). All hybridization and washing conditions were performed as specified by the manufacturer. Quantitation of the bands was performed using Odyssey software. Fold increase was determined by first normalizing each band against GAPDH and then dividing that number by the value of the normalized control.

PARP Western. DU145 cells were plated at a density of 3.0×10^6 cells per 150 mm^2 plate and treated 24 h later with either DMSO or **10ae**. The cells were collected at the indicated time points, and cell pellets were frozen. The frozen cell pellets were lysed in 1% NP40/PBS lysis buffer containing protease inhibitors. Equal amounts of total cellular protein was then resolved on a 10%-SDS-polyacrylamide gel. The gels were transferred onto nitrocellulose paper (S/S), hybridized with anti-PARP antibodies (BD), and developed using ECL (Perkin-Elmer, MA) solution.

Tubulin Polymerization. MAP-rich tubulin form bovine brain (Cytoskeleton), resuspended in PEM (80 mM PIPES, (pH 6.9), 0.5 mM EGTA, 2 mM $MgCl_2$) was preincubated with drug or its vehicle dimethyl sulfoxide at room temperature for 5 min. PEG containing GTP was added to start the tubulin polymerization reaction. The reaction was monitored by a spectrophotometer at OD350 nm at 37 °C. The final concentrations of tubulin and GTP were 1.15 mg/mL and 4 mM, respectively.

Tubulin Staining. HeLa cells were grown on glass coverslips and treated with **10ae** (0.25 μM, 0.5 uM), paclitaxel (0.005 μM), or vincristine (0.005 μM) for 18 h. The coverslips were washed in phosphate buffered saline and fixed in freshly prepared 4% paraformaldehyde. The cells were blocked and permeabilized and stained with 1:400 dilution of anti-α-tubulin conjugated with FITC (Sigma) followed by staining with DAPI (0.5 ug/mL). The coverslips were mounted onto glass slides using Prolong Gold Antifade (Molecular Probes/InVitrogen, CA) solution and visualized using an Olympus IX-71 inverted fluorescent microscope at 100× magnification. The cells were photographed using the DP-71 camera system using two filters followed by merging and representative merged images are shown.

AUTHOR INFORMATION

Corresponding Author

*For M.V.R.R.: phone, (212) 659-6875; fax, (215) 893-6989; E-mail, r.reddy@mssm.edu. For E.P.R.: phone, (212) 659-5571; E-mail, ep.reddy@mssm.edu.

Author Contributions

§These authors contributed equally.

Notes

The authors declare the following competing financial interest(s): Dr. E.P. Reddy is a stockholder, Board member, grant recipient and paid consultant of Onconova Therapeutics Inc. Dr. M.V.R. Reddy is a stockholder and paid consultant of Onconova Inc. Dr. S. Cosenza is a paid consultant of Onconova Therapeutics Inc.

ACKNOWLEDGMENTS

This work was supported by grants from the NIH (CA 109820) and Onconova Therapeutics Inc.

ABBREVIATIONS USED

MSA, microtubule-stabilizing agents; GTP, guanosine triphosphate; FACs, fluorescence-activated cell sorting; PLK-1, Polo-like kinase-1; Bcl-2, B-cell lymphoma-2; MAPS, microtubule-associated proteins; GAPDH, glyceraldehyde 3-phosphate dehydrogenase; PARP, poly(ADP-ribose)polymerase

REFERENCES

(1) Downing, K. H.; Nogales, E. Tubulin and microtubule structure. *Curr. Opin. Cell Biol.* **1998**, *10*, 16−22.

(2) Jordan, A.; Hadfield, J. A.; Lawrence, N. J.; McGown, A. T. Tubulin as a target for anticancer drugs: agents which interact with the mitotic spindle. *Med. Res. Rev.* **1998**, *18*, 259−296.

(3) Hamel, E. Antimitotic natural products and their interactions with tubulin. *Med. Res. Rev.* **1996**, *16*, 207−231.

(4) (a) Siemann, D. W.; Bibby, M. C.; Dark, G. G.; Dicker, A. P.; Eskens, F. A. L. M.; Horsman, M. R.; Marme, D.; LoRusso, P. M. Differentiation and definition of vascular targeted-therapies. *Clin. Cancer Res.* **2005**, *11*, 416−420. (b) Siemann, D. W. *Vascular-Targeted Therapies in Oncology*; John Wiley & Sons: New York, 2006. (c) Gaya, A. M.; Rustin, G. J. Vascular disrupting agents: A new class of drug in cancer therapy. *Clin. Oncol.* **2005**, *17*, 277−290. (d) Tozer, G. M.; Kanthou, C.; Baguley, B. C. Disrupting tumor blood vessels. *Nature Rev. Cancer* **2005**, *5*, 423−435. (e) Lippert, J. W., III. Vascular disrupting agents. *Bioorg. Med. Chem.* **2007**, *15*, 605−615.

(5) (a) Chaplin, D. J.; Horsman, M. R.; Siemann, D. W. Current developments status of small-molecule vascular disrupting agents. *Curr. Opin. Invest. Drugs* **2006**, *7*, 522−528. (b) Tron, G. C.; Pirali, T.; Sorba, G.; Pagliai, F.; Busacca, S.; Genazzani, A. A. Medicinal chemistry of combretastatin A4: present and future directions. *J. Med. Chem.* **2006**, *49*, 3033−3044. (c) Li, Q.; Sham, H. L. Discovery and development of mitotic agents that inhibit polymerization for the treatment of cancers. *Expert Opin. Ther. Pat.* **2002**, *12*, 1663−1702. (d) Nam, N. H. Combretastatin A4 analogues as antimitotic antitumor agents. *Curr. Med. Chem.* **2003**, *10*, 1697−1722. (e) Hsieh, H. P.; Liou, J. P.; Mahindroo, N. Pharmaceutical design of antimitotic agents based on combretastatin. *Curr. Pharm. Des.* **2005**, *11*, 1655−1677. (f) Mahindroo, N.; Liou, J. P.; Chang, J. Y.; Hsieh, H. P. Antitubulin agents for the treatment of cancer—a medicinal chemistry updates. *Expert. Opin. Ther. Pat.* **2006**, *16*, 647−691. (g) Tron, G. C.; Pagliai, F.; Del Grosso, E.; Genazzani, A. A.; Sorba, G. Synthesis and cytotoxic evaluation of combretafurazans. *J. Med. Chem.* **2005**, *48*, 3260−3268. (h) Pirali, T.; Busacca, S.; Beltrami, L.; Imovilli, D.; Pagliai, F.; Miglio, G.; Massarotti, A.; Verotta, L.; Tron, G. C.; Sorba, G.; Genazzani, A. A. Synthesis and cytotoxicity evaluation of combretafuran, potential scaffolds for dual-action antitumor agents. *J. Med. Chem.* **2006**, *49*, 5372−5376. (i) Zhang, Q; Peng, Y.; Wang, X. I.; Keenan, S. M.; Arora, S.; Welsh, W. J. Highly potent triazole-based tubulin polymerization inhibitors. *J. Med. Chem.* **2007**, *50*, 749−754.

(6) Pinney, K. G.; Bounds, A. D.; Dingeman, K. M.; Mocharla, V. P.; Pettit, G. R.; Bai, R.; Hamel, E. A new anti-tubulin agent containing the benzo[*b*]thiophene ring system. *Bioorg. Med. Chem. Lett.* **1999**, *9*, 1081−1086.

(7) Flynn, B. L.; Hamel, E.; Jung, M. K. One pot synthesis of benzo[*b*]furan and indole inhibitors of tubulin polymerization. *J. Med. Chem.* **2002**, *45*, 2670−2673.

(8) Wang, L.; Woods, K. W.; Li, Q.; Barr, K. J.; McCroskey, R. W.; Hannick, S. M.; Gherke, L.; Credo, R. B.; Hui, Y. H.; Marsh, K.; Warner, R.; Lee, J. Y.; Zielinski-Mozng, N.; Frost, D.; Rosenberg, S. H.; Sham, H. L. Potent, oral active heterocycle-based combretastatin C-4 analogues: synthesis, structure−activity relationship, pharmacokinetics, and in vivo antitumor activity evaluation. *J. Med. Chem.* **2002**, *45*, 1697−1711.

(9) Niher, Y.; Suga, Y.; Morinaga, Y.; Akiyama, Y.; Tsuji, T. Syntheses and antitumor activity of cis-restricted combretastatins: 5-membered heterocyclic analogues. *Bioorg. Med. Chem. Lett.* **1998**, *8*, 3153−3158.

(10) Szczepankiewicz, B. G.; Liu, G.; Jae, H. S.; Tasker, A. S.; Gunawardana, I. W.; von Geldern, T. W.; Gwaltney, S. L., II; Wu-Wong, J. R.; Gehrke, L.; Chiou, W. J.; Credo, R. B.; Alder, J. D.; Nukkala, M. A.; Zielinski, N. A.; Jarvis, K.; Mollison, K. W.; Frost, D. J.; Bauch, J. L.; Hui, Y. H.; Claiborne, A. K.; Li, Q.; Rosenberg, S. H. New mitotic agents with activity in multidrug-resistant cell lines and in vivo efficacy in murine tumor models. *J. Med. Chem.* **2001**, *44*, 4416−4430.

(11) Mahboobi, S.; Pongratz, H.; Hufsky, H.; Hockemeyer, J.; Frieser, M.; Lyssenko, A.; Paper, D. H.; Bürgermeister, J.; Böhmer, F. D.; Fiebig, H. H.; Burger, A. M.; Baasner, S.; Beckers, T. Synthetic 2-aryolindole derivatives as new class of potent inhibitory, antimitotic agents. *J. Med. Chem.* **2001**, *44*, 4535−4553.

(12) (a) Liou, J. P.; Chang, Y. L.; Kuo, F. M.; Chang, C. W.; Tseng, H. Y.; Wang, C. C.; Yang, Y. N.; Chang, J. Y.; Lee, S. J.; Hsieh, H. P. Concise synthesis and structure−activity relationships of combretastatin A-4 analogues, 1-aroylindoles, 3-aroylindoles, a novel classes of potent antitubulin agent. *J. Med. Chem.* **2004**, *47*, 4247−4257. (b) Liou, J. P.; Mahindroo, N.; Chang, C. W.; Guo, F. M.; Lee, S. W. H; Tan, U. K.; Yeh, T. K.; Kuo, C. C.; Chang, Y. W.; Lu, P. H.; Tung, Y. S.; Lin, K. T.; Chang, J. Y.; Hsieh, H. P. Structure−activity relationship studies of 3-aroylindole as potent antitmitotic agents. *ChemMedChem* **2006**, *1*, 1106−1118.

(13) Martino, G. D.; Edler, M. C.; Regina, G. L.; Coluccia, A.; Barbera, M. C.; Barrow, D.; Nicholson, R. I.; Chiosis, G.; Brancale, A.; Hamel, E.; Artico, M.; Silvestri, R. New arylthioindoles: potent inhibitors of tubulin polymerization. 2. Structure−activity relationships and molecular modeling studies. *J. Med. Chem.* **2006**, *49*, 947−954.

(14) Bacher, G.; Nickel, B.; Emig, P.; Vanhoefer, U.; Seeber, S.; Shandra, A.; Klenner, T.; Beckers, T. D-24851, a novel synthetic microtubule inhibitor, expressive curative antitumoral activity in vivo, shows efficacy toward multidrug-resistant tumor cells and lacks neuorotoxicity. *Cancer Res.* **2001**, *61*, 392−399.

(15) Bhalla, K.; Ibrado, A. M.; Tourkina, E.; Tang, C.; Mahoney, M. E.; Chang, Y. Taxol induces internucleosomal DNA fragmentation associated with programmed cell death in human myeloid leukemia cells. *Leukemia* **1993**, *7*, 563−568.

(16) Jordan, M. A. Mechanism of action of antitumor drugs that interact with microtubules and tubulin. *Curr. Med. Chem. Anti-Cancer Agents* **2002**, *2*, 1−17.

(17) Schiff, P. B.; Fant, J.; Horwitz, S. B. Promotion of microtubule assembly in vitro by taxol. *Nature* **1979**, *277*, 665−667.

(18) Schiff, P. B.; Horwitz, S. B. Taxol stabilizes microtubules in mouse fibroblast cells. *Proc. Natl. Acad. Sci. U.S.A.* **1980**, *77*, 1561−1565.

(19) Bollag, D. M.; McQueney, P. A.; Zhu, J.; Hensens, O.; Koupal, L.; Liesch, J.; Goetz, M.; Lazarides, E.; Woods, C. M. Epothilones a new class of microtubule-stabilizing agents with a taxol-like mechanism of action. *Cancer Res.* **1995**, *55*, 2325−2333.

(20) Ter Haar, E.; Kowalski, R. J.; Hamel, E.; Lin, C. M.; Longely, R. E.; Gunasekara, S. P.; Rosenkranz, H. S.; Day, D. W. Discodermolide a cytotoxic marine agent that stabilizes microtubules more potently than taxol. *Biochemistry* **1996**, *35*, 243−250.
(21) Stephen, J. H.; Thomas, U. M.; David, T. M.; Rejza, F.; Randall, W. K.; Timothy, J. M.; Stuart, L. S. Dissecting cellular processes using small molecules: identification of colichicine-like, taxol-like and other small molecules that perturb mitosis. *Chem. Biol.* **2000**, *7*, 275−286.
(22) Yasushi, S.; Toshimasa, T.; Yukimasa, N. GS-164, a small synthetic compound, stimulates tubulin polymerization by a similar mechanism to that of Taxol. *Cancer Chemother. Pharmacol.* **1997**, *40*, 513−520.
(23) Molander, G. A.; George, K. M.; Monovich, L. G. Total synthesis of (+)-Isoschizaandrin utilizing a samarium(II) iodide-promoted 8-endo ketyl-olefin cyclization. *J. Org. Chem.* **2003**, *68*, 9533−9540.
(24) Harker, W. G.; Sikic, B. I. Multidrug (pleiotropic) resistance in doxorubicin selected variants of the human sarcoma cell lines MES-SA. *Cancer Res.* **1985**, *45*, 4091−4096.
(25) Patricia, K; Andrew, E. P.; Tao, L.; Buzz, B. Moesin controls cortical rigidity, cell rounding and spindle morphogenesis during mitosis. *Curr. Biol.* **2008**, *18*, 91−101.
(26) Lanzi, C.; Cassinelli, G.; Cuccuru, G.; Supino, R.; Zuco, V.; Ferlini, C.; Scambia, G.; Zunino, F. Cell cycle checkpoint efficiency and cellular response to paclitaxel in prostate cancer cells. *Prostate* **2001**, *48*, 254−264.
(27) Nawab, A.; Thakur, V. S.; Yunus, M.; Ali, M, A.; Gupta, S. Selcetive cell cycle arrest and induction of apoptosis in human prostate cancer cells in polyphenol-rich extract in solanum ingrum. *Int. J. Mol. Med.* **2001**, *29*, 277−284.
(28) Jeffrey, H. W.; Zhaozong, Z.; Jun, G.; Ann, R. K.; Levy, K. Establishment of human cancer cell clones with different characteristics: a model for screening chemo-preventive agents. *Anticancer Res.* **2007**, *27*, 1−16.
(29) Kiranmai, G.; Ramana Reddy, M. V.; Stephen, C. C.; Boominathan, R.; Stacy, J. B.; Nabisa, P.; Jiandong, J.; James, H.; Premkumar, E. P. ON1910, a non-ATP competitive small molecule inhibitor of PLK1, is a potent cancer agent. *Cancer Cell* **2005**, *7*, 275−286.
(30) Hendzel, M. J.; Wei, Y.; Mancini, M. A.; Van Hooser, A.; Ranalli, T.; Brinkley, B. R.; Bazett-Jones, D. P.; Allis, C. D. Mitosis-specific phosphorylation of histone H3 initiates primarily within pericentromeric heterochromatin during G2 and spreads in an ordered fashion coincident with mitotic chromosome condensation. *Chromosoma* **1997**, *10*, 348−360.
(31) Van Hooser, A.; Goodrich, D. W.; Allis, C. D.; Brinkley, B. R.; Mancini, M. A. HistoneH3 phosphorylation is required for the initiation, but not maintenance, of mammalian chromosome condensation. *J. Cell Sci.* **1998**, *111*, 3497−3506.
(32) Prigent, C.; Dimitrov, S. Phosphorylation of serine 10 in histone H3, what for? *J. Cell Sci.* **2003**, *116*, 3677−3685.
(33) Coleman, K. E.; Brat, D. J.; Cotsonis, G. A.; Lawson, D.; Cohen, C. Proliferation (MIB-1 expression) in oligodendrogliomas: assessment of quantitative methods and prognostic significance. *Appl. Immunohistochem. Mol. Morphol.* **2006**, *14*, 109−114.
(34) Ling, Y. H.; Tornos, C.; Perez-Soler, R. Phosphorylation of Bcl-2 is a marker of M phase events and not a determinant of apoptosis. *J. Biol. Chem.* **1998**, *273*, 18984−18991.
(35) Nurse, P. Universal control mechanism regulating onset of M-phase. *Nature* **1990**, *344*, 503−508.
(36) King, R. W.; Jackson, P. K.; Kirschner, M. W. Mitosis in transition. *Cell* **1994**, *79*, 563−571.
(37) Golesteyn, R. M.; Schultz, S. J.; Bartek, J.; Ziemiecki, A.; Ried, T.; Nigg, E. A. Cell cycle analysis and chromosomal localization of human Plk1, a putative homologue of the mitotic kinases *Drosophila polo* and *Saccharomyces cerevisiae* Cdc5. *J. Cell Sci.* **1994**, *107*, 1509−1517.
(38) Chan, G. K.; Jablonski, S. A.; Sudakin, V.; Hittle, J. C.; Yen, T. J. Human BUBR1 is a mitotic checkpoint kinase that monitors CENP-E functions at kinetochores and binds the cyclosome/APC. *J. Cell Biol.* **1999**, *146*, 941−954.
(39) Birk, M.; Burkle, A.; Pekari, K.; Maier, T.; Schmidt, M. Cell cycle dependent cytotoxicity and mitotic spindle checkpoint dependency of investigational and approved anti-mitotic agents. *Int. J. Cancer* **2011**, *130*, 798−807.
(40) Soldani, C.; Scovassi, A. I. Poly (ADP-ribose) polymerase-1 cleavage during apoptosis: an update. *Apoptosis* **2002**, *7*, 321−328.